Author(s): Lautaoja, Juulia H.; O'Connell, Thomas; Mäntyselkä, Sakari; Peräkylä, Juuli; Kainulainen, Heikki; Pekkala, Satu; Permi, Perttu; Hulmi, Juha J.

Title: Higher glucose availability augments the metabolic responses of the C2C12 myotubes to exercise-like electrical pulse stimulation

Year: 2021

Version: Accepted version (Final draft)

Please cite the original version:

Lautaoja, J. H., O'Connell, T., Mäntyselkä, S., Peräkylä, J., Kainulainen, H., Pekkala, S., Permi, P., & Hulmi, J. J. (2021). Higher glucose availability augments the metabolic responses of the C2C12 myotubes to exercise-like electrical pulse stimulation. American Journal of Physiology : Endocrinology and Metabolism, 321(2), E229-E245. https://doi.org/10.1152/ajpendo.00133.2021

Higher glucose availability augments the metabolic responses of the C2C12 myotubes to exercise-like electrical pulse stimulation

Lautaoja JH[1*], O´Connell TM[2#], Mäntyselkä S[3#], Peräkylä J[3], Kainulainen H[1], Pekkala S[1#], Permi P[3,4#], Hulmi JJ.[1*]

[1]Faculty of Sport and Health Sciences, NeuroMuscular Research Center, University of Jyväskylä, Jyväskylä, Finland: *juulia.h.lautaoja@jyu.fi*; *heikki.s.o.kainulainen@jyu.fi*; *satu.p.pekkala@jyu.fi*; *juha.hulmi@jyu.fi*

[2]Department of Otolaryngology-Head & Neck Surgery, Indiana University School of Medicine, Indianapolis, USA: *thoconne@iu.edu*

[3]Department of Biological and Environmental Science, University of Jyväskylä, Jyväskylä, Finland: *sakari.a.mantyselka@student.jyu.fi*; *juuli.v.perakyla@jyu.fi*; *perttu.permi@jyu.fi*

[4]Department of Chemistry, Nanoscience Center, University of Jyväskylä, Jyväskylä, Finland

Keywords: acetate, exerkine, metabolomics, skeletal muscle, branched chain fatty acids

[*]Correspondence to Juulia Lautaoja: *juulia.h.lautaoja@jyu.fi* and Juha Hulmi: *juha.hulmi@jyu.fi*, Faculty of Sport and Health Sciences, NeuroMuscular Research Center, University of Jyväskylä, Jyväskylä, Finland.

[#]Equal contribution.

Supplementary Material available: 10.6084/m9.figshare.14376413.

ABSTRACT

The application of exercise-like electrical pulse simulation (EL-EPS) has become a widely used exercise mimetic *in vitro*. EL-EPS produces similar physiological responses as *in vivo* exercise, while less is known about the detailed metabolic effects. Routinely the C2C12 myotubes are cultured in high glucose medium (4.5 g/l), which may alter EL-EPS responses. In this study, we evaluate the metabolic effects of EL-EPS under the high and low glucose (1.0 g/l) conditions to understand how substrate availability affects the myotube response to EL-EPS.

The C2C12 myotube, media and cell-free media metabolites were analyzed using untargeted nuclear magnetic resonance (NMR)-based metabolomics. Further, translational and metabolic changes and possible exerkine effects were analyzed. EL-EPS enhanced substrate utilization as well as production and secretion of lactate, acetate, 3-hydroxybutyrate and branched chain fatty acids (BCFAs). The increase in BCFAs correlated with branched chain amino acids (BCAAs) and BCFAs were strongly decreased when myotubes were cultured without BCAAs suggesting the action of acyl-CoA thioesterases on BCAA catabolites. Notably, not all EL-EPS responses were augmented by high glucose because EL-EPS increased phosphorylated c-Jun N-terminal kinase and interleukin-6 secretion independent of glucose availability. Administration of acetate and EL-EPS conditioned media on HepG2 hepatocytes had no adverse effects on lipolysis or triacylglycerol content.

Our results demonstrate that unlike in cell-free media, the C2C12 myotube and media metabolites were affected by EL-EPS, particularly under high glucose condition suggesting that media composition should be considered in future EL-EPS studies. Further, acetate and BCFAs were identified as putative exerkines warranting more research.

New and Noteworthy. The present study examined for the first time the metabolome of 1) C2C12 myotubes, 2) their growth media and 3) cell-free media after exercise-like electrical pulse stimulation under distinct nutritional loads. We report that myotubes grown under high glucose conditions had greater responsiveness to EL-EPS when compared to lower glucose availability conditions and increased media content of acetate and branched chain fatty acids suggests they might act as putative exerkines warranting further research.

INTRODUCTION

Adequate physical activity is known to prevent and treat many diseases, such as metabolic, cardiovascular and musculoskeletal disorders (1). During exercise, muscles secrete molecules that can act as intra- (autocrine and paracrine) or inter-tissue (endocrine) signaling factors (2). These muscle-derived signaling mediators have been recently shown to promote for instance muscle-liver crosstalk during and after exercise, which is essential for many physiological processes, such as regulation of energy metabolism during increased fuel demand (3, 4). Overall, recognition of the skeletal muscle as a secretory organ (5, 6) has opened a new research area in exercise physiology.

Pedersen and colleagues originally named muscle-originated proteins and cytokines as myokines (7). Afterwards, Tarnopolsky and colleagues (8) defined exerkines as myokines and other molecules, such as metabolites, extracellular vesicles and nucleic acids, secreted from the contracting muscles (*i.e* myometabokiome (9)) and other tissues. Due to the large size (30-40% of the body mass) and great vascularization, contribution of the skeletal muscle to the secreted myokine/exerkine pool is significant (10). A number of *in vivo* studies have been conducted including analyses of a variety of body fluids (11-13) and muscle tissues as well as examination of arteriovenous difference (14) to examine muscle-derived molecules during rest and exercise. However, these analyses will include molecules secreted from other organs in the body so that metabolic products of skeletal muscle cannot be specified.

In order to look specifically at skeletal muscle metabolism with exercise, we have used a widely adopted cell culture model to mimic *in vivo* exercise *in vitro.* This model involves treating the C2C12 myotubes with exercise-like electrical pulse stimulation (hereafter EL-EPS as recommended (15)), which has been shown to produce similar physiological responses at transcriptional, translational and metabolic levels as *in vivo* exercise (for review, see (15, 16)). A major benefit of the *in vitro* EL-EPS approach is the ability to selectively and exclusively study myotube metabolism and myotube-derived molecules.

Although nutrition is a critical factor that regulates skeletal muscle response to exercise, *in vitro* studies have largely overlooked the composition of the media (17). Indeed, a recent study showed that the media composition had a major effect on the analyzed metabolite profiles of different cell lines (18). Thus, to raise awareness of this aspect, we examined the effects of two media containing different amounts of glucose and EL-EPS on myotube metabolism. Because the glucose content in routine cell culture medium may differ from normal/healthy physiological range (19), it is important to determine how the metabolic functioning of myotubes after EL-EPS is affected by the glucose availability.

In the present study, we aimed to assess the effects of EL-EPS and nutritional status (glucose availability) on C2C12 myotube metabolism by conducting untargeted NMR-based metabolomics analysis of both the cell extract and the media. To roughly estimate whether metabolite uptake or release was occurring, we also analyzed cell-free media controls. The latter was analyzed also after EL-EPS to exclude the possible direct effects of EL-EPS on the media. Altogether, our results show that the glucose availability affected a significant number of the observed metabolic changes in response to EL-EPS suggesting that nutrient availability is indeed a critical factor that should be taken into account in the future studies.

MATERIALS AND METHODS

Cell cultures. Murine C2C12 myoblasts and human HepG2 hepatocytes were purchased from ATCC (Manassas, VA, USA). The myoblasts were grown and differentiated as previously described (20). Briefly, the myoblasts were seeded on 6-well plates (NunclonTM Delta; Thermo Fisher Scientific, Waltham, MA, USA) at a density of approximately 12 000 cells/cm^2. The growth medium (GM) contained high glucose (HG, 4.5 g/l) Dulbecco´s Modified Eagle Medium (DMEM, #BE12-614F, Lonza, Basel, Switzerland), 10% (v/v) fetal bovine serum (FBS, #10270, Gibco, Rockville, MD, USA), 100 U/ml penicillin and 100 µg/ml streptomycin (P/S, #15140, Gibco) and 2 mM L-glutamine (#25030, Gibco). The differentiation medium (DM) contained HG DMEM supplemented with 5 % (v/v) FBS, 100 U/ml and 100 µg/ml P/S and 2 mM L-glutamine. The HG DM was refreshed every two days, except at day 4 post differentiation the cells were acclimatized to low glucose (LG, 1 g/l, #BE12-707F, Lonza) DM if the following experiments were conducted in LG conditions. According to the medium provider, the only difference between the DMEMs used is the glucose content. The C2C12 experiments were conducted at days 4-6 post-differentiation in 2 ml of medium. The cells were tested negative for mycoplasma (MycoSPY, M020-025, Biontex Laboratories GmbH, München, Germany). The HepG2 cells were grown in HG DMEM/Glutamax medium (#31266, Gibco) supplemented with 10 % (v/v) FBS and 100 U/ml and 100 µg/ml P/S. The cells were seeded on 10 cm^2 dishes (NunclonTM Delta; Thermo Fisher Scientific) at a density of approximately 9000 cells/cm^2. The HepG2 cells experiments were conducted in 5 ml of serum-and antibiotic-free medium. All the cell experiments were performed below passage number 9 (C2C12) or 12 (HepG2) in a humidified environment at 37 °C and 5 % CO_2.

EL-EPS protocols for C2C12 myotubes. Comparable low frequency EL-EPS protocol as used in the present study has previously been reported to induce similar metabolic and translational changes as *in vivo* exercise (21-23). According to the studies by Nikolić and colleagues (16) along with visible contractions verified under a microscope (results not shown), the 24-hour chronic low frequency EL-EPS protocol (1 Hz, 2 ms, 12 V) was chosen. On day 6 post differentiation, all C2C12 samples were collected immediately after the cessation of the EL-EPS.

EL-EPS for metabolomics, on day 5 post C2C12 differentiation, the wells were rinsed with phosphate buffered saline (PBS, #10010, Gibco) and serum-free (SF) HG or LG DMEM supplemented with 2 mM L-glutamine was added for 1 hour (24). The medium was removed, the wells were rinsed with PBS and fresh SF HG or LG DMEM supplemented with 2 mM L-glutamine was added. The chronic low frequency EL-EPS was applied by placing the C-Dish carbon electrodes attached to C-Pace EM machine (IonOptix Corporation, Milton, MA, USA) to the wells. To roughly elucidate whether the cells possibly take up or release metabolites, we analyzed the metabolome of the cell-free LG and HG media supplemented with 2 mM L-glutamine. As recommended previously (18), the cell-free media were treated identical to the cell-containing samples as they were also incubated for 24 hours with and without EL-EPS (*i.e.* no cells/no power and no cells/power), N = 3 (Supplementary Material Table S1, Figure S2).

EL-EPS for oleate oxidation, the cells were first acclimatized to dissolved and albumin-complexed 0.1 mM oleic acid (#O3008, oleic acid-albumin from bovine serum, Sigma-Aldrich, St. Luis, MO, USA) and 1 mM L-carnitine (C0158, Sigma-Aldrich) in either SF LG or HG DMEM supplemented with 2 mM L-glutamine on the day 4 post differentiation. The next day, the electrodes were placed directly to the wells and EL-EPS was applied as described above. The measurement of oleate oxidation was carried out for 2 h at 37 °C as previously described (25) with slight modifications. Briefly, at differentiation day 6, after 22 hours of stimulation, EL-EPS was paused, the media were collected and centrifuged for 1 min at 1000 x g before storing at -80 °C. The cells were rinsed with PBS and fresh SF HG or LG DMEM supplemented with 2 mM L-glutamine, 0.1 mM oleic acid, 1 mM L-carnitine and 1 μCi/ml [9,10-^{3}H(N)] oleic acid (24 Ci/mmol, NET289005MC, PerkinElmer, Boston, MA, USA) was added. The radiolabeled oleic acid was omitted from the negative controls. The EL-EPS was applied for the remaining 2 hours. The

^{1}H Nuclear magnetic resonance (NMR) spectroscopy. The cell lysates and the experiment media (including cell-free controls) were collected and prepared for the ^{1}H NMR analysis as described (26) with slight modifications. Briefly, samples form three wells were pooled to ensure adequate metabolite concentrations per one ^{1}H NMR measurement. Media from three wells were mixed with cold methanol (600 μl sample and 1200 μl methanol) and cells were scraped into 200 μl of 90 % (v/v) 9:1 aqueous methanol/chloroform mixture. The resulting supernatants were stored at -80 °C before room temperature lyophilisation using vacuum concentrator (Speed Vac plus SC110 A Savant Instruments Inc., Farmingdale, NY, USA) equipped with a vacuum pump (Vacuum pump V-700, Büchi, Flawil, Switzerland) and controller (Vacuum Controller V-850, Büchi). The experiments were replicated independently three times, total N = 6–8 per group.

^{1}H NMR data collection and analysis. The samples lyophilized at RT were reconstituted as previously described (26) with slight modifications. In brief, Na_2HPO_4-NaH_2PO_4 buffer (150 mM, pH = 7.4) in 99.8% D_2O (Acros Organics™, Thermo Fisher Scientific) containing 0.5 mM 3-(trimethylsilyl) propanesulfonic-d6 acid sodium salt (DSS-d6, IS-2 Internal Standard, Chenomx, Edmonton, Canada) was used for reconstitution. The samples were placed in 3 mm round bottom NMR sample tubes (Norell Inc., Morganton, NC, USA) for analysis. All the NMR spectra were collected using a Bruker AVANCE III HD NMR spectrometer, operating at 800 MHz ^{1}H frequency (Bruker Corporation, MA, USA) equipped with a cryogenically cooled ^{1}H, ^{13}C, ^{15}N triple-resonance probehead. The temperature of the samples was set at 25 °C during the measurements. For the ^{1}H one-dimensional (1D) NOESY experiments, the FID was sampled with 133926 points covering the spectral width of 16741 Hz, using a relaxation delay of 5 s, acquisition time of 4 s, and mixing time of 0.1 s. The signal was accumulated with 128 scans. The obtained data was analyzed using Chenomx 8.5-8.6 software (Chenomx). In addition to ^{1}H 1D spectra, heteronuclear ^{1}H-^{13}C single quantum coherence spectroscopy (HSQC) and ^{1}H-^{13}C HSQC-*to*tal *c*orrelation *s*pectroscop*y* (HSQC-TOCSY), as well as homonuclear ^{1}H-^{1}H TOCSY and ^{1}H-^{1}H *d*ouble *q*uantum *f*iltered *co*rrelation *s*pectroscop*y* (DQF-COSY) two-dimensional (2D) spectra were used to confirm the identification of the profiled metabolites. The TopSpin 4.0.9 software (Bruker Corporation) was used for processing and analysis of the 2D spectra. The spike in-analyses of isobutyric acid (#I1754, Sigma-Aldrich), isovaleric acid (#129542, Sigma-Aldrich) were included.

Oleate oxidation. After the EL-EPS, the media were run through ion-exchange columns containing Dowex-OH- resin (pH 7, 1X8-200, Cat no. 217425, Sigma Aldrich) (25). Deionized H_2O was used to elute the $^{3}H_2O$, which originates from intracellular [9,10-^{3}H(N)] oleic acid β-oxidation that was further secreted to the media. The radioactivity was analyzed as disintegration per minute (DPM) in Optiphase HiSafe 3 scintillation cocktail (Cat no. 1200.437, PerkinElmer) with Tri-Carb 2910 TR Liquid Scintillation Analyzer (PerkinElmer). The results were calculated using PerkinElmer equations (https://www.perkinelmer.com/fi/lab-products-and-services/application-support-knowledgebase/radiometric/radiochemical-calculations.html). The cells were washed twice with PBS and harvested for total protein content analysis as previously described (20) except for centrifugation at 13 000 x g for 10 min at +4 °C. The oleate oxidation results were normalized against total protein content and the experiments were replicated independently three times, total N = 8–10 per group.

HepG2 hepatocyte experiments. Normal and steatotic HepG2 hepatocytes were used in the experiments. Based on our dose-response experiment steatosis, *i.e.* fat accumulation, was induced by 24-hour administration of 500 μM oleic acid (#03008, Sigma-Aldrich) in serum- and antibiotic-free conditions when compared to the non-exposed hepatocytes (Supplementary Material Figure S1). The acetate (sodium acetate, CAS No. 127-09-3, Merck, Darmstadt, Germany) dose-response experiment in steatotic hepatocytes suggested that a greater dose (3 mM) than was observed in ^{1}H NMR analysis (1.5 mM) had no additional effect on intracellular triacylglycerol content over the lower dose (Supplementary Material Figure S1).

The normal and steatotic hepatocytes were administered with EL-EPS-stimulated or unstimulated C2C12 conditioned medium (CM) or alternatively with or without 1.5 mM acetate. The C2C12 cells were treated as described for the HG ^{1}H NMR analysis above. After EL-EPS, the media of the stimulated and unstimulated cells were collected and centrifuged for 5 min at 217 x g RT to remove cell debris before administration on hepatocytes. In another set of experiments, 1.5 mM acetate or equivalent volume of PBS was administered on both normal and steatotic hepatocytes in serum- and antibiotic-free DMEM/Glutamax. After the 24-hour incubation, triacylglycerol extraction from the hepatocytes was conducted. Briefly, the media were collected, centrifuged for 5 min at 217 x g, RT and stored at -80 ˚C until use. The HepG2 cells were washed and scraped into PBS, while subsamples for the measurement of total protein content were homogenized into previously described buffer (20). Next, 2:1 methanol-chloroform mixture was added to PBS-cell suspension followed by 5 min centrifugation at 724 x g, RT. The supernatant was transferred into a new tube and chloroform, 50 mM citric acid and H_2O were added. Methanol and chloroform phases were separated by centrifugation for 10 min at 724 x g, RT. Chloroform phase was collected and evaporated at +70 °C using SpeedVac Concentrator (Thermo Fisher Scientific). The resulting lipid pellet was dissolved into ethanol before measurement. The content of intracellular triacylglycerol as well as glycerol and cytokines in the media were measured as described below.

Measurement of intracellular total protein content, enzyme activities and media glycerol content. Total protein content (Bicinchoninic Acid Protein Assay Kit, Pierce

Biotechnology, Rockford, IL, USA), triacylglycerol (#981786, Thermo Fisher Scientific) and glycerol (#984316, Thermo Fisher Scientific) concentrations as well as lactate dehydrogenase (LDH) (#981906, Thermo Fisher Scientific) and citrate synthase (CS) (#CS0720, Sigma-Aldrich) enzyme activities were measured with an automated Konelab or Indiko plus analyzer (Thermo Fisher Scientific). All assays were conducted according to manufacturer´s protocols and enzyme activities in the cells were normalized against total protein content.

4-plex cytokine ELISA analyses. The C2C12 and HepG2 media were centrifuged for 1 min at 1000 x g or 5 min at 217 x g, respectively, at +4 °C and resulting supernatants were stored at -80 °C until use. Next, 25 µl of the samples were directed to mouse (Q-Plex Mouse 4-plex Cytokine Panel (#115549MS, Quansys Biosciences, North West, UT, USA) or human 4-plex Cytokine Panel (Q-Plex Human Cytokine High Sensitivity, #112533HU, Quansys Biosciences) assay that were conducted according to the manufacturer's protocols. In the murine assay, the limit of detection for interleukin-1β (IL-1β) was 12.41 pg/ml, for IL-6 2.90 pg/ml, for tumor necrosis factor α (TNF-α) 3.40 pg/ml and for interferon γ (IFN-γ) 5.40 pg/ml. In the human assay, the limit of detection for IL-4 was 0.02 pg/ml, for IL-6 0.30 pg/ml, for IL-10 2.39 pg/ml and for IFN-γ 0.09 pg/ml.

Protein extraction and Western blot. The cells were harvested for western blot and enzyme activity analysis as previously described (20) except for centrifugation at 13 000 x g for 10 min at +4 °C. The western blot was conducted as previously described (20). Briefly, 10 µg of total protein per samples were loaded on 4–20% Criterion™ TGX Stain-Free™ protein gels (#5678094, Bio-Rad Laboratories, Hercules, CA, USA) and samples were separated by SDS-PAGE. To visualize proteins using stain-free technology, the gels were activated and the proteins were transferred to the PVDF membranes followed by blocking and overnight probing with primary antibodies at +4 °C (27). Enhanced chemiluminescence (SuperSignal west femto maximum sensitivity substrate; Pierce Biotechnology, Rockford, IL, USA) and ChemiDoc MP device (Bio-Rad Laboratories) were together used for protein visualization. Stain free (whole lane) was used as a loading control and for the normalization of the results. Primary antibodies used in the present study were purchased from Cell Signaling Technology: $p38^{Thr180/Tyr182}$ (#4511), p38 (#9212), $ERK1/2^{Thr202/Tyr204}$ (#9101), ERK1/2 (#9102), $SAPK/JNK1/2^{Thr183Tyr185}$ (#4668) and SAPK/JNK (#9252). The horseradish peroxidase-conjugated secondary IgG antibody was purchased from Jackson ImmunoResearch Laboratories, PA, USA.

Statistical analyses. The two-way multivariate analysis of variance (two-way MANOVA) was used to analyze main and interaction effects, while the group comparisons were conducted by using multivariate Tukey´s test unless stated otherwise (IBM SPSS Statistics, version 26 for Windows, SPSS Chicago, IL, USA). The Spearman´s correlation coefficient was used to analyze correlations (SPSS). The VIsualization and Integration of Metabolomics Experiments (VIIME) software (https://viime.org, (28)) was used to generate the heat maps and principal components analyses. The results are presented as means ± SEM. The level of significance was set at $P < 0.05$.

RESULTS

EL-EPS yielded different metabolic responses under LG and HG conditions

We studied the effects of chronic low frequency EL-EPS and medium glucose content on the metabolism of C2C12 myotubes using untargeted ^{1}H NMR-based metabolomics analysis of the conditioned media and cell extracts. The cell-free media controls were incubated 24 hours with and without EL-EPS. This allowed us to show that EL-EPS does not induce changes in the metabolite profiles in the cell-free media (Supplementary Material Figure S2 and Table S1). The principal component analysis (PCA) of the metabolite profiles demonstrated that the four study groups were clearly separated, especially in the media (Figure 1A). Interestingly, in the PCA of the media, the first principal component separates the groups based on glucose levels and the second principal component separates them based on the application of EL-EPS (Figure 1A).

The NMR-based metabolomics analysis resulted in identification of 47 individual metabolites. More specifically, we quantified 39 metabolites from the cells and 37 metabolites from the media and the reporting threshold (*i.e.* the metabolite was detected in over 50 % of cases) was met by 37 and 34 metabolites, respectively (Supplementary Material Table S2). Among the cells and the media, 24 metabolites were shared (Figure 1B). Overall, the heat map clustering of the metabolites quantified from the cells and media demonstrated that the stimulation-induced differences in the metabolites between LG and HG conditions were greater in the latter, especially in the cells (Figure 1D-E). The hierarchical cluster analysis of heat maps from the cell extracts suggests that the metabolites clustered into three categories including those responsive to EL-EPS and to distinct media glucose contents, while in the media more categories were observed (Figure 1D-E).

Similar to a previous study (12), most of the identified metabolites were distributed among four biological groups. These were (i) metabolism of energy related metabolites (creatine, carbohydrates and TCA cycle intermediates; 14 metabolites), (ii) short and branched chain fatty acids (SCFAs and BCFAs, respectively) and ketone bodies (six metabolites), (iii) amino acids and related metabolites (24 metabolites) as well as (iv) vitamins and others (three metabolites) (Figure 1C, for individual metabolites, see Supplementary Material Table S2). In the cells, 18 metabolites were altered due to either EL-EPS or medium glucose content (*i.e.* EPS and HG main effects, respectively), while eight metabolites demonstrated an interaction effect (EPS x HG) (Supplementary Material Table S3). In the media, EPS had a main effect on 17 and HG on 13 metabolites, while the interaction effect was detected in seven metabolites (Supplementary Material Table S3).

Glycolytic ATP production and acetate responded strongly to EL-EPS

During the EL-EPS, the glucose content in the media decreased when compared to cell-free media indicating increased consumption to support the contraction-induced increase in the energy demand in the cells (Figure 2A). Simultaneously, lactate content increased both in the cells and in the media, while the level of phosphocreatine decreased and dephosphorylated creatine increased suggesting that both glycolytic and phosphocreatine energy sources were utilized (Figure 2B-D). In agreement with the increased lactate production and secretion in our experiments, the lactate dehydrogenase (LDH) activity was increased in the cells after EL-EPS, especially in the HG condition (Figure 2E). Finally, we observed an increase in the cell and media content of acetate, a short chain fatty acid (SCFA) that can act as a potential fuel source during exercise (29). It appears that in the resting C2C12 cells the net uptake of acetate was enhanced based on substantially lower acetate content in the cell media than in the cell-free media (LG or HG vs. cell-free LG or HG, Student´s *t*-test, $P < 0.001$, Figure 2F). In contrast, during EL-EPS acetate secretion exceeded its uptake partly due to the increased cellular production, at least in HG condition (HG+EPS vs. cell-free HG+EPS, Student´s *t*-test, $P < 0.05$, Figure 2F). The effect of the increased glycolysis in response to EL-EPS was accompanied by unaltered content of citrate, the first TCA cycle intermediate, and unaltered citrate synthase (CS) enzyme activity, while the levels of the intermediates observed later in the cycle including succinate, fumarate and malate, were increased in the cells in HG condition (Figure 3A-E).

Increased intracellular amino acid levels after EL-EPS

Overall, amino acids were more affected by the EL-EPS than by the glucose availability and only minor effects were observed between HG and LG conditions. The Figure 4A shows a forest plot of the amino acids with the $\log_2$ fold changes of the metabolites in response to EL-EPS shown along the x-axis (for individual amino acid box plots, see Supplementary Material Figure S3). The plot shows the levels of each of the amino acids under both LG and HG conditions. A set of seven amino acids were increased and eight remained unchanged in response to EL-EPS in the cells, while in the media five amino acids increased, two decreased and ten remained unaltered (Figure 4B). In contrast, a shared increasing HG effect was observed in three amino acids in the cells and media, while a decreasing HG effect was observed in one and two amino acids, respectively (Figure 4C). The contents of cysteine (Student´s *t*-test, media vs. cell-free media, $P < 0.01$), glycine ($P < 0.001$), histidine ($P < 0.05$) and lysine ($P < 0.001$) were lower in the cell-free than in the cell-containing media suggesting release of these amino acids from the C2C12 cells and for cystine and lysine release appears to be further increased during EL-EPS (Supplementary Material Figure S3). In contrast, serine ($P < 0.001$) and glutamine ($P < 0.001$) contents were greater in the cell-free media controls suggesting active uptake of these amino acids by the C2C12 cells and this appears to be further increased during EL-EPS (Supplementary Material Figure S3).

Increased intra- and extracellular contents of branched chain fatty acids after EL-EPS

A set of branched chain fatty acids (BCFAs) demonstrated significant increases induced by EL-EPS. The levels 2-methylbutyrate, isobutyrate and isovalerate were increased in the media after EL-EPS independent of the glucose availability showing their release/secretion from the cells (BCFAs were not detected from the cell-free media) (Figure 5A-C). Of these BCFAs, isobutyrate and isovalerate were also increased in the cells after EL-EPS, but this was explained by the increase in HG condition (Figure 5A-C). Indeed, the responses of BCFAs to EL-EPS were overall greater in HG condition. The observation of the BCFAs was unanticipated and the source of these metabolites was not entirely clear. Based simply upon chemical structure, we suspected that these metabolites could be the result of branched chain amino acid (BCAA) catabolism. To test this, we evaluated the correlations between the BCFAs and the BCAAs. As shown in supplementary Table S4, we found no significant correlations in the media, but very strong correlations were found between the BCAA and BCFAs in the cells. The Figure 5D postulates the pathway through which the BCAAs are transformed.

To unequivocally confirm the identity of the BCFAs, we conducted spike-in ^{1}H NMR experiments, where authentic standards of these compounds were added to the samples to show that the spectral patterns were clearly matching. Finally, we also confirmed by culturing the C2C12 myotubes in BCAA-free media that indeed, BCFAs appear to originate from the BCAA breakdown based on their greater abundance in standard BCAA containing media (pilot results, Supplementary Material Figure S3).

Increased ketone body levels in the media after EL-EPS

The ketone body 3-hydroxybutyrate was identified in the cell-free and the C2C12 media (Figure 5E). It should be noted that the signals for 3-hydroxybutyrate in the cell-free and unstimulated media samples were near the limit of detection and thus the quantitation is only approximate. Application of EL-EPS led to a significant increase in the signals for 3-hydroxybutyrate in the C2C12 media enabling confident identification and quantitation. The increase in 3-hydroxybutyrate content was greater under HG condition demonstrating that ketone body production in these cells was affected by the glucose availability.

Glucose availability resulted in variable changes in exercise and stress associated markers

As the glucose content together with the EL-EPS influenced the metabolite levels, we investigated next whether this was also translated to the phosphorylation levels of the mitogen-activated protein kinases (MAPKs) that are common markers of skeletal muscle after energetic stress and exercise (30). We observed that EL-EPS increased the phosphorylation of stress-activated protein kinase/c-Jun N-terminal kinase (SAPK/JNK)$^{Thr184/Tyr185}$ independent of the glucose availability (Figure 6A), while the phosphorylation of p38$^{Thr180/Tyr182}$ and extracellular regulated kinase (ERK1/2)$^{Thr202/Tyr204}$ remained unaltered (Supplementary Material Figure S4). Because SAPK/JNK has been shown to regulate IL-6 signaling in the C2C12 myotubes after EL-EPS (31), we examined the common exercise-responsive cytokines from the media and found that only IL-6 was detectable after EL-EPS. The IL-6 concentration was increased independent of the glucose availability (Figure 6B). Further, Hojman and colleagues showed that IL-6 release from the muscle cells is at least in part dependent on the lactate production (32) and similarly our correlation analysis demonstrated a positive association between the media IL-6 content and the content of lactate in the cells ($r = 0.551$, $P < 0.01$), and in the media ($r = 0.660$, $P < 0.001$). For the full list of the IL-6 and metabolite correlations, see Supplementary Material Table S4.

The changes in the metabolites in response to EL-EPS suggests that the C2C12 cell line is very glycolytic in nature even under low frequency stimulation and therefore in addition to the unaltered activity of the citrate synthase as a TCA cycle marker (Figure 3E), we expected that the fatty acid oxidation might not increase. To test this hypothesis, oleic acid and L-carnitine acclimatized C2C12 myotubes were applied with 24-hour EL-EPS during which radiolabeled [9,10-^{3}H(N)] oleic acid was added together with unlabeled oleic acid and L-carnitine in fresh media. The rate of oleate oxidation was analyzed as the amount of ^3H_2O produced and secreted by the myotubes to the culture media. Indeed, the analysis of the metabolic effects of EL-EPS demonstrated that oleate oxidation even decreased in the cells under HG condition (Figure 6C). This occurred without EL-EPS-induced changes in triacylglycerol content, although media glycerol content as a marker of lipolysis was increased in HG condition after EL-EPS (Figure 6D-E).

EL-EPS has no effect on cell viability but myotubes grown in HG may be more viable

To understand whether the myotubes were more viable and thus perhaps more metabolically active in the HG condition, which could partly explain some of the observed results, LDH enzyme activity was measured from the media as a marker of cell rupture (16) (Supplementary Material Figure S5). Overall, the cell viability remained unaffected by the EL-EPS protocol. However, LDH activity tended to be lower in HG condition in NMR-experiments thus suggesting possibly better viability than in LG condition (Supplementary Material Figure S5).

Potential myotube-derived exerkines had little effect on normal and steatotic hepatocytes

An initial goal of this study was to search for potential, myotube-derived metabolites that could act as exerkines. To test whether myotube-derived exerkines can alter hepatic steatosis, we cultured HepG2 hepatocytes and induced the accumulation of triacylglycerol by supplementation of the media with oleic acid (Supplementary Material Figure S1). Steatosis was not accompanied with inflammation because inflammatory markers (IL-4, IL-6, IL-10 and INF-γ) in the media remained below the detection limit (data not shown). As acetate was the metabolite secreted with the largest fold change in response to EL-EPS, we administrated normal and steatotic hepatocytes with 1.5 mM acetate or with EL-EPS CM. The acetate concentration was chosen based on the ^{1}H NMR analysis results. After the 24-hour incubation, we observed that neither of the approaches had adverse effects on the triacylglycerol content of the hepatocytes or the glycerol content in the media (Figure 7A-D). That said, the level of glycerol in the media as a marker of lipolysis approached an increasing trend after EL-EPS CM administration (EPS main effect, $P = 0.098$, Figure 7D).

DISCUSSION

Skeletal muscle metabolism is known to increase dramatically from rest to exercise and the ability of the cells to adapt to increased energy demand is vital (33). In agreement with these known *in vivo* physiological facts and similar to previous *in vivo* studies (11, 12, 34), we observed a number of perturbations to energy metabolism that were affected by EL-EPS. Our studies also observed a significant impact of nutrient availability on the EL-EPS-induced metabolic changes. Most, but not all of the EL-EPS responses were of larger magnitude in high glucose conditions, which may be due to the fact that in low glucose condition the 24-hour EL-EPS almost completely depleted media and cells from glucose. The decreased glucose content in the media after EL-EPS is in line with previous studies demonstrating that EL-EPS promotes glucose uptake into the myotubes (16) and the well-known fact that exercise *in vivo* increases glucose uptake into the skeletal muscle (35). Similarly, in agreement with *in vitro* (16) and *in vivo* (36) findings, we observed an increased production and secretion of lactate and decreased intracellular content of phosphocreatine demonstrating that the applied EL-EPS induced glycolytic ATP production and energy demands in the C2C12 myotubes. Indeed, the C2C12 cell line has been considered to be glycolytic in nature (37) and rely on anaerobic glycolysis at rest (38), which may explain the increased lactate production and decreased fat oxidation during the applied low frequency EL-EPS. As lactate plays an important role in intercellular signaling of nearby and/or distant cells (39), its role as an exerkine has probably been underappreciated and should be further studied.

Our studies revealed alterations in a set of short and branched chain fatty acids (S/BCFAs) and ketone bodies with EL-EPS. SCFAs such as acetate, propionate and butyrate are commonly observed with *in vivo* studies and are common products of gut microbial metabolism (40), while also other tissues can produce SCFAs. For example, Van Hall and colleagues showed that exercise increased leg acetate release by 9-fold when compared with rest (41). In the present study, we showed that intra- and extracellular contents of acetate were increased after EL-EPS, while the former was more pronounced in high glucose condition. During increased energy demand or restricted TCA cycle function, all of the pyruvate-derived acetyl-CoA might have not successfully entered the TCA cycle and thus the excess can be hydrolyzed to acetate and released into the circulation (42, 43). Acetate can be produced from pyruvate via enzymatic and non-enzymatic reactions including pyruvate dehydrogenase (PDH) and reactive oxygen species (ROS) (44), respectively, and PDH activity (45) and ROS levels (16) are increased by exercise and/or myotube contractions. In addition, hyperactive glucose metabolism and nutritional excess have been related to incomplete metabolism and excretion of metabolites, which lead to promoted conversion of pyruvate to acetate (44). This might have been the case also in our study since in high glucose condition the accumulation of succinate, fumarate and malate suggests that substrate availability and entry to the TCA cycle might have exceeded the capacity of the oxidative phosphorylation machinery thus resulting in incomplete substrate oxidation. It is possible that the reduced need for full TCA cycle activity is due to enhanced glycolysis, which may provide enough ATP for the working myotubes based on the strongly increased lactate levels.

As acetate has been shown to positively modify liver lipid metabolism (46), the effects of myotube-derived acetate and the whole EPS secretome (EL-EPS CM) on hepatocytes were examined. By applying acetate and EL-EPS CM to normal and steatotic hepatocytes, we found that the intracellular triacylglycerol content in the hepatocytes remained unaltered in the studied conditions. However, the molecules originated from the contracted muscle cells (EL-EPS CM) had a tendency for increased lipolysis in the hepatocytes, inferred from the increased media content of glycerol. In long term, this could lead to reduced intracellular triacylglycerol content, but further studies are needed. Also more studies investigating dose-response effects of acetate are also warranted. This is because we found high levels of acetate from the cell-free media controls similar to previous study (47), meaning that hepatocyte culture already had high levels of acetate before further adding it into the media. Future physiology studies should also investigate whether the high levels of acetate use and release from muscle cells have physiological effects *in vivo*.

Besides acetate, the media content of 3-hydroxybutyrate, a common ketone body, increased after EL-EPS and the response was greater in high glucose condition. Previously, an increased content of circulating 3-hydroxybutyrate after exercise has been considered to act as a biomarker of metabolic shift from the utilization of carbohydrates towards fats (34) and SCFAs and ketone bodies have been reported to positively modify lipid, carbohydrate and protein metabolism in the muscle and in other tissues (48). Although 3-hydroxybutyrate has been considered to be produced mainly by the liver, the growing body of evidence demonstrates that during exercise skeletal muscle could secrete certain ketone bodies and thus contribute to the circulating ketone body pool (13). The 3-hydroxybutyrate has been detected in the muscle interstitial fluid after exercise (13), and the enzyme regulating 3-hydroxybutyrate synthesis, HMG-CoA synthase (*HMGCS2*), has been shown to be elevated in skeletal muscle after exercise (49). Additionally, 3-hydroxybutyrate dehydrogenase

(*BDH1*), which converts acetoacetate into 3-hydroxybutyrate has been shown to be increased in the skeletal muscle by exercise and decreased by inactivity ((49), https://metamex.com). Thus, 3-hydroxybutyrate could be an exerkine, however, further studies are needed to verify its functions on the whole-body metabolism and crosstalk after exercise.

In addition to the more routinely observed SCFAs, we observed a set of unique changes in several BCFAs including 2-methylbutyrate, isobutyrate and isovalerate that all increased after EL-EPS. Correlations between BCFAs and BCAAs along with studies using BCAA depleted media strongly indicate that the BCFAs are indeed derived from BCAA catabolism. Previous *in vivo* study suggested that during exercise BCFA precursors derived from the BCAA catabolism were increased in the skeletal muscle (50) and identified from the circulation (51). Concordant with this finding, we demonstrated that BCFAs can be produced and released by muscle cells in response to EL-EPS. Further, we simultaneously observed an increase in the BCAAs in the cells after EL-EPS, identical as reported in glycolytic human type II-muscle fibers after exercise (52). Previous studies have shown that increased levels of circulating BCAAs and decreased BCAA degradation has been associated with poor metabolic health (53). In this study, we reported i) unaltered media BCAA content, ii) increased content of BCAA breakdown products and iii) increased intracellular content of many amino acids (including BCAAs) after EL-EPS. Together these results suggest that the EL-EPS perhaps enhanced protein breakdown and amino acid recycling similarly as *in vivo* exercise (54). In summary, high correlations of the BCAAs and their breakdown products as well as very low levels of BCFAs in the experiment with BCAA depleted media support the evidence that in the C2C12 cells the origin of BCFAs seems to be BCAA catabolism.

The enzymes needed for the conversion of the acyl-CoA derivatives originated from the BCAA catabolism (2-methylbutyryl-CoA, isobutyryl-CoA and isovaleryl-CoA (55)) into 2-methylbutyrate, isobutyrate and isovalerate may include acyl-CoA thioesterases (ACOTs), of which skeletal muscle expresses different isoforms (56) and the C2C12 cell line at least *Acot3* and *Acot9* (57). The ACOT9 isoform has been shown to have a unique substrate specificity with the ability to hydrolyze short-chain acyl-CoA esters, including isobutyryl-CoA and isovaleryl-CoA (56, 58). This further suggests that the mitochondrial link between branched chain fatty acid and amino acid metabolism could be ACOT9 (58).

The effect of EL-EPS on the amino acids was consistently greater than the high glucose effect both in the cells and in the media. The *in vivo* changes in the circulating amino acids have been reported to be controversial and dependent on their specific glucogenic vs. ketogenic, non-essential vs. essential or other properties (11, 12) as well as exercise intensity (59). To summarize, although our results are mainly in agreement with recent *in vivo* systematic reviews on exercise metabolomics (11, 12), more research is needed to better understand the stimulation-induced changes in myotube and media metabolites. Indeed, the number of studies analyzing the metabolome after EL-EPS is small (60) and, to best of our knowledge, this study is the first to study metabolites after EL-EPS under distinct nutritional loads.

We observed a decline in oleate oxidation during EL-EPS under high glucose condition, while under low glucose condition the decrease approached a trend. Decreased oleate oxidation may be related to the above-mentioned i) incomplete oxidation of the energetic intermediates during hyperactive metabolism and nutrient overloading (44) and ii) glycolytic nature of the C2C12 cell line (37). Addition of the fresh media containing the radiolabeled and unlabeled oleic acid in right proportion is an essential step for accurate oxidation measurement when using our protocol. Based on our results, the 24-hour EL-EPS almost completely depleted the glucose from the media in LG condition. In oleate oxidation experiments, we had to replace the EL-EPS media with the fresh ^{3}H oleic acid-containing media after 22 hours of stimulation and thus, we simultaneously provided the cells with fresh glucose for the remaining 2 hours of the EL-EPS. This may have temporarily stimulated the cells to rely heavily on glucose, perhaps, at least in LG condition. Further, increased glycolysis causes accumulation of acetyl-CoA that could inhibit β-oxidation via downregulation of β-ketoacyl-CoA thiolase (61). That said, because acetyl-CoA cannot be transported across membrane, the excess might also be transformed to acetate via the action of ACOT enzymes (58) or via non-enzymatic processes (44) and then secreted from the cells to balance the intracellular state of TCA cycle substrates (42) as we observed in the present study. Besides decreased oleate oxidation, we observed no changes in intracellular triacylglycerol content similar to Laurens and colleagues (62), although our observation of the increased glycerol release may be associated with enhanced lipolysis under high glucose condition after EL-EPS. Additionally, contraction-induced changes in triacylglycerol content may be pre-treatment specific because acclimatization of the C2C12 myotubes to fatty acids has been shown to cause intramyocellular triacylglycerol accumulation, which was prevented by short-duration low frequency EL-EPS (63). Moreover, previous studies have reported controversial results on fatty acid oxidation after EL-EPS and the main factors affecting the rate of β-oxidation seem to be related to the stimulation protocol, duration of the measurement, fatty acid analyzed (*e.g.* oleate or palmitate), analysis protocol/method and the cell line used (37, 38, 63-66).

In addition to changes in the metabolome, the applied EL-EPS altered the phosphorylation and secretion of stress-inducible markers, such as MAPKs and cytokines, commonly analyzed after *in vivo* exercise and *in vitro* EL-EPS (16). The phosphorylation of SAPK/JNK increased after EL-EPS independent of glucose availability, which is supported by *in vivo* studies demonstrating that glycolytic exercise increases SAPK/JNK phosphorylation (67, 68). Of the exercise-responsive cytokines, we observed an increase in the secretion of IL-6 after EL-EPS, also independent of glucose availability. Interestingly, muscle IL-6 secretion may occur in part through proteasome-dependent release initiated by lactate production (32). Indeed, the IL-6 in the media correlated positively with the intra- and extracellular lactate content in the present study (Supplementary Material Table S4). Additionally, SAPK/JNK has been shown to regulate IL-6 metabolism (31) and indeed we observed that IL-6 and phosphorylated SAPK/JNK responded similarly to EL-EPS.

Strengths of the study. To the best of our knowledge, the present study is the first to examine and compare the intra- and extracellular metabolome of myotubes after EL-EPS. Importantly, although we did not use tracers, we included analysis of the cell-free media controls with or without EL-EPS to the present study. This enabled us to roughly estimate whether the metabolites were taken up to the cells or released into the media. Moreover, these cell-free controls also validated the experiments showing that the effects of EL-EPS on media metabolite levels were most probably through myotube contractions and not through unspecific effects of EL-EPS on media. In addition, the number of studies analyzing the effects of glucose availability on the myotube metabolism after EL-EPS is surprisingly small (21), although the nutritional status is known to regulate many intracellular processes even under non-exercising conditions (69). That said, the limitation of the existing literature is that not all studies have clearly reported the medium glucose content (*e.g.* only a few of the EL-EPS articles reviewed by Nikolić and colleagues (16)) although it is highly recommended in other *in vitro* studies (17, 70). Overall, our study improves understanding of the role of nutrient availability on the metabolic changes induced by EL-EPS.

Limitations of the study. In the present study, the selected metabolomics platform (^{1}H NMR) provided an introductory insight into the differences in the C2C12 myotube and media metabolites, while future studies using mass spectrometry (MS)-based metabolomics would be beneficial for the analysis of lower abundance metabolites. Indeed, combination of the NMR and MS platforms in metabolomics research has been recommended (71). Moreover, studies using dynamic turnover of metabolomics (*i.e.* fluxomics (72)) are warranted to investigate the flux of the metabolites *in vitro* and *in vivo*. We also acknowledge that we detected some minor differences between LG and HG DMEMs in some metabolites in addition to glucose (Supplementary Material Table S1), but unlike myo-inositol that is derived from glucose, those are likely explained by batch-to-batch differences. Finally, time series data collection after different modes of EL-EPS in upcoming studies would provide a broader understanding of the metabolite characteristics in recovery phase both in the cells and in the media.

CONCLUSION

By using the C2C12 myotubes we found that EL-EPS enhanced energy source utilization as well as production and secretion of lactate, acetate and BCFAs (see summary in Figure 8). Many of the EL-EPS induced changes in the myotube and/or media metabolites, such as contents of lactate, acetate, BCFAs and TCA cycle intermediates, were affected by the glucose availability. This is possibly at least in part because low glucose condition almost fully depleted glycolytic C2C12 cells from glucose in 24 hours. Thus, we recommended to consider the effect of nutrition and the choice of media in future EL-EPS studies. Lastly, the novel increase in BCFAs with EL-EPS leads to the enticing notion that these metabolites may act as exerkines warranting more research on their physiological significance and regulation by *in vivo* exercise.

GRANTS

This work was funded by the Academy of Finland (Grant No. 298875 to H.K, 308042 to S.P., 323435 to P.P and 275922 to J.J.H.). T.M.O. is supported by grants from National Institutes of Health, National Institute of Arthritis and Musculoskeletal and Skin Diseases (P01AG039355 and P30AR072581) as well as the Additional Ventures, Single Ventricle Research Fund.

DISCLOSURES

No conflicts of interest, financial or otherwise, are declared by the authors.

ACKNOWLEDGEMENTS

We thank Hannah Crossland, Jouni Tukiainen and Eija Laakkonen for their help with the EL-EPS setup. Mika Silvennoinen, Ulla Sahinaho and Jari Ylänne are thanked for their suggestions and help regarding the oleate oxidation experiments. We appreciate the help received from Maarit Lehti and Emilia Lähteenmäki with methodological issues and Hanne Tähti and Mervi Matero are thanked for their help in sample collection. We thank Susanna Luoma, Tanja Toivanen and Jukka Hintikka for helping with the sample and data analysis.

AUTHOR CONTRIBUTIONS

J.H.L., S.P and J.J.H. designed the study. J.H.L, drafted the manuscript, prepared images, conducted the cell experiments, data analysis and statistics, S.M. conducted the ^{1}H NMR cell experiments, S.M. and P.P. performed the ^{1}H NMR measurements, S.M. and T.M.O. analyzed the ^{1}H NMR data, J.P. conducted the oleate oxidation cell experiments and data analysis, S.P. assisted with the hepatocyte experiments, H.K. provided resources and guidance, T.M.O, S.P. and J.J.H guided the preparation of the manuscript. All authors have approved the final version of the manuscript.

FIGURE LEGENDS

FIGURE 1. The principal component analysis (PCA), Venn diagram and heat map visualizations of the altered metabolites in response to exercise-like electrical pulse stimulation (EL-EPS). (A) The PCA score plots. Fold changes were logarithmically transformed ($\log_2$) and pareto scaling was used to create the plots. (B) The applied EL-EPS altered 37 and 35 metabolites in the C2C12 cells and in the media, respectively, and of these 24 metabolites were common among groups. (C) The identified metabolites were distributed among four biological groups. The heat map categorization (*k*-means clustering) of the analyzed metabolites in (D) the cells and (E) in the media. The dashed lines cluster the metabolites that respond similarly to EL-EPS or to media glucose content. Heat map coloring is based on z-scores. N = 6–8 per group. SCFAs = short chain fatty acids, BCFAs = branched chain fatty acids, AAs = amino acids, LG/HG = low/high glucose condition, LG/HG + EPS = EL-EPS in low/high glucose condition.

FIGURE 2. EL-EPS increased energy utilization via glycolytic pathways and readily available energy stores. (A) Glucose, (B) lactate (C) dephosphorylated creatine and (D) phosphocreatine contents in the C2C12 cells and/or in the media. (E) Lactate dehydrogenase (LDH) enzyme activity in the cells. (F) Acetate content. * and *** = $P < 0.05$ and $P < 0.001$, respectively. N = 6–8 per group. The two-way MANOVA was used to analyze the effects of

the applied EL-EPS and media glucose content (EPS and HG effects, respectively) and their interaction effect, while group comparisons were analyzed with multivariate Tukey´s test. In A and F, the dashed lines represent the levels of the cell-free LG and HG media controls (*i.e.* mean of the stimulated and non-stimulated media). Lack of the dashed lines refers to the undetected metabolite content from the cell-free media controls.

FIGURE 3. Increase in the content of tricarboxylic acid (TCA) cycle intermediates in the C2C12 cells after EL-EPS was dependent on medium glucose availability. The contents of (A) citrate, (B) succinate, (C) fumarate and (D) malate. (E) Citrate synthase (CS) enzyme activity in the cells. * and *** = $P < 0.05$ and $P < 0.001$, respectively. N = 6–8 per group. The two-way MANOVA was used to analyze the effects of the applied EL-EPS and media glucose content (EPS and HG effects, respectively) and their interaction effect, while group comparisons were analyzed with multivariate Tukey´s test.

FIGURE 4. The effects of EL-EPS on the analyzed amino acids was greater than the effect of the glucose availability. Forest plots of the amino acids (A) in the C2C12 cells and (B) in the medium analyzed as logarithmically transformed fold changes (Log_2 (FC)), N = 6–8 per group. The error bars demonstrate 95 % confidence intervals of the analyzed groups (LG and LG + EPS or HG and HG + EPS). Next to the plots are shown the interaction effect (EPS x HG) and the main effects of the applied EL-EPS (EPS) and media glucose content (HG) analyzed by the two-way MANOVA. If the interaction effect is significant, the main effects are shown in the brackets. Multivariate Tukey´s test was used to analyze the group comparisons and significant results are depicted as larger dots. Red = low glucose samples, blue = high glucose samples. Grey arrows depict the direction (increase or decrease) of the main effect. Pie charts of the amino acids demonstrating (B) EPS and (C) HG main effects in the cells and in the medium. Of note: the 95 % confidence intervals were calculated based on Student´s t-distribution, while the group comparisons were conducted using more stringent Tukey´s test.

FIGURE 5. The production and secretion of branched chain fatty acids (BCFAs) and ketone bodies were increased after EL-EPS independent of the glucose availability. The contents of (A) 2-methylbutyrate, (B) isobutyrate and (C) isovalerate. (D) Schematic presentation of the branched chain amino acids and their breakdown metabolites, BCFAs. The content of (E) ketone body 3-hydroxybutyrate in the media. *, ** and *** = $P < 0.05$, $P < 0.01$ and $P < 0.001$, respectively. N = 6–8 per group. The two-way MANOVA was used to analyze the

effects of the applied EL-EPS and media glucose content (EPS and HG effects, respectively) and their interaction effect, while group comparisons were analyzed with multivariate Tukey´s test. ACOT9 = Acyl-CoA thioesterase 9. In E, the dashed lines represent the level of the cell-free LG and HG media controls (*i.e.* mean of the no cells/no power and co cells/power content). Lack of the dashed lines refers to the undetected metabolite content from the cell-free media controls.

FIGURE 6. EL-EPS promoted protein phosphorylation and cell metabolism especially under HG condition. (A) Phosphorylated stress-activated protein kinase/c-Jun N-terminal kinase (SAPK/JNK1/2)$^{Thr183/Tyr185}$, total SAPK/JNK1/2 and representative blots. - = no stimulation, + = stimulation. In the figure, the values are presented as normalized to LG = 1 or HG = 1. (B) Interleukin-6 (IL-6) concentration in the media, (C) oleate oxidation rate, (D) intracellular triacylglycerol (TG) content and (E) media glycerol content. *, ** and *** = $P < 0.05$, $P < 0.01$ and $P < 0.001$, respectively. In A and D-E, N = 6, in B = 12 (pool of the ^{1}H NMR and oleate oxidation (22-hour time-point) experiments) and in C, N = 8–10 per group. The two-way MANOVA was used to analyze the effects of the applied EL-EPS and media glucose content (EPS and HG effects, respectively) and their interaction effect, while group comparisons were analyzed with multivariate Tukey´s test.

FIGURE 7. The 24-hour administration of acetate and conditioned medium from the stimulated C2C12 cells had only minor effects on normal and steatotic HepG2 hepatocytes. (A) Cell triacylglycerol and (B) media glycerol contents after administration of 1.5 mM acetate (diluted in PBS) or PBS control. (C) Cell triacylglycerol and (D) media glycerol contents after administration of the media from the stimulated or unstimulated C2C12 cells grown under high glucose conditions (EPS and CTRL medium, respectively). N = 3 per group. The two-way MANOVA was used to analyze the effects of the applied EL-EPS and steatosis (EPS and health effects, respectively) and their interaction effect, while group comparisons were analyzed with multivariate Tukey´s test.

FIGURE 8. Summary of the effects of EL-EPS on C2C12 myotube metabolism. The application of EL-EPS increased ATP production pathways, including glycolysis and lipolysis. The resulting pyruvate and acetyl-CoA were converted to lactate by lactate dehydrogenase (LDH) and to acetate possibly through reactive oxygen species (ROS) and pyruvate dehydrogenase (PDH). A buildup of several TCA intermediates suggests an overall reduction in oxidative metabolism. This is also consistent with the observed reduction in fatty

acid oxidation suggested by the reduce oleate metabolism. The intermediates of the BCAA catabolism include 2-methylbutyrate, isobutyrate and isovalerate that are in part produced by the acyl-CoA thioesterases (ACOTs), possibly ACOT9. These BCAA breakdown products belong to the branched chain fatty acids (BCFAs) and they can be directed to the TCA cycle, production of ketone bodies (*e.g.* 3-hydroxybutyrate) or as we observed they might also be released out of the cells. Blue = decreased, red = increased, bold black = unchanged and black = undetected content.

REFERENCES

1. **Pedersen BK and Saltin B.** Exercise as medicine - evidence for prescribing exercise as therapy in 26 different chronic diseases. *Scand.J.Med.Sci.Sports* 25: 1-72, 2015.

2. **Fiuza-Luces C, Garatachea N, Berger NA and Lucia A.** Exercise is the real polypill. *Physiology* 28: 5, 330-358, 2013.

3. **Whitham M, Parker BL, Friedrichsen M, Hingst JR, Hjorth M, Hughes WE, Egan CL, Cron L, Watt KI and Kuchel RP.** Extracellular Vesicles Provide a Means for Tissue Crosstalk during Exercise. *Cell metabolism* 27: 1, 237-251. e4, 2018.

4. **Castaño C, Mirasierra M, Vallejo M, Novials A and Párrizas M.** Delivery of muscle-derived exosomal miRNAs induced by HIIT improves insulin sensitivity through down-regulation of hepatic FoxO1 in mice. *Proceedings of the National Academy of Sciences* 117: 48, 30335-30343, 2020.

5. **Febbraio MA and Pedersen BK.** Contraction-induced myokine production and release: is skeletal muscle an endocrine organ? *Exerc.Sport Sci.Rev.* 33: 3, 114-119, 2005.

6. **Pedersen BK and Febbraio MA.** Muscles, exercise and obesity: skeletal muscle as a secretory organ. *Nature Reviews Endocrinology* 8: 8, 457, 2012.

7. **Pedersen BK, Steensberg A, Fischer C, Keller C, Keller P, Plomgaard P, Febbraio M and Saltin B.** Searching for the exercise factor: is IL-6 a candidate? *Journal of Muscle Research & Cell Motility* 24: 2-3, 113, 2003.

8. **Safdar A, Saleem A and Tarnopolsky MA.** The potential of endurance exercise-derived exosomes to treat metabolic diseases. *Nature Reviews Endocrinology* 12: 9, 504, 2016.

9. **Weigert C, Lehmann R, Hartwig S and Lehr S.** The secretome of the working human skeletal muscle—A promising opportunity to combat the metabolic disaster? *PROTEOMICS–Clinical Applications* 8: 1-2, 5-18, 2014.

10. **Piccirillo R.** Exercise-induced myokines with therapeutic potential for muscle wasting. *Frontiers in physiology* 10: 287, 2019.

11. **Sakaguchi CA, Nieman DC, Signini EF, Abreu RM and Catai AM.** Metabolomics-Based Studies Assessing Exercise-Induced Alterations of the Human Metabolome: A Systematic Review. *Metabolites* 9: 8, 164, 2019.

12. **Schranner D, Kastenmüller G, Schönfelder M, Römisch-Margl W and Wackerhage H.** Metabolite Concentration Changes in Humans After a Bout of Exercise: a Systematic Review of Exercise Metabolomics Studies. *Sports medicine-open* 6: 1: 11, 2020.

13. **Zhang J, Bhattacharyya S, Hickner RC, Light AR, Lambert CJ, Gale BK, Fiehn O and Adams SH.** Skeletal muscle interstitial fluid metabolomics at rest and associated with an exercise bout: application in rats and humans. *American Journal of Physiology-Endocrinology and Metabolism* 316: 1, E43-E53, 2018.

14. **Murphy RM, Watt MJ and Febbraio MA.** Metabolic communication during exercise. *Nature metabolism* 1-12, 2020.

15. **Carter S and Solomon TP.** In vitro experimental models for examining the skeletal muscle cell biology of exercise: the possibilities, challenges and future developments. *Pflügers Archiv-European Journal of Physiology* 471: 3, 413-429, 2019.

16. **Nikolić N, Görgens SW, Thoresen GH, Aas V, Eckel J and Eckardt K.** Electrical pulse stimulation of cultured skeletal muscle cells as a model for in vitro exercise–possibilities and limitations. *Acta physiologica* 220: 3, 310-331, 2017.

17. **Lagziel S, Gottlieb E and Shlomi T.** Mind your media. *Nature metabolism* 1-4, 2020.

18. **Daskalaki E, Pillon NJ, Krook A, Wheelock CE and Checa A.** The influence of culture media upon observed cell secretome metabolite profiles: The balance between cell viability and data interpretability. *Anal.Chim.Acta* 1037: 338-350, 2018.

19. **Emerging Risk Factors Collaboration.** Diabetes mellitus, fasting blood glucose concentration, and risk of vascular disease: a collaborative meta-analysis of 102 prospective studies. *The Lancet* 375: 9733, 2215-2222, 2010.

20. **Lautaoja JH, Pekkala S, Pasternack A, Laitinen M, Ritvos O and Hulmi JJ.** Differentiation of murine C2C12 myoblasts strongly reduces the effects of myostatin on intracellular signaling. *Biomolecules* 10: 695, 2020.

21. **Farmawati A, Kitajima Y, Nedachi T, Sato M, Kanzaki M and Nagatomi R.** Characterization of contraction-induced IL-6 up-regulation using contractile C2C12 myotubes. *Endocr.J,* EJ12-0316, 2012.

22. **Evers-van Gogh IJ, Alex S, Stienstra R, Brenkman AB, Kersten S and Kalkhoven E.** Electric pulse stimulation of myotubes as an in vitro exercise model: cell-mediated and non-cell-mediated effects. *Scientific reports* 5: 10944, 2015.

23. **Son YH, Lee S, Lee SH, Yoon JH, Kang JS, Yang YR and Kwon K.** Comparative molecular analysis of endurance exercise in vivo with electrically stimulated in vitro myotube contraction. *J.Appl.Physiol* 127: 1742-1753, 2019.

24. **Furuichi Y, Manabe Y, Takagi M, Aoki M and Fujii NL.** Evidence for acute contraction-induced myokine secretion by C2C12 myotubes. *PLoS One* 13: 10, e0206146, 2018.

25. **Wang H, Kuusela S, Rinnankoski-Tuikka R, Dumont V, Bouslama R, Ramadan UA, Waaler J, Linden A, Chi N and Krauss S.** Tankyrase inhibition ameliorates lipid disorder via suppression of PGC-1α PARylation in db/db mice. *Int.J.Obes.* 44: 8: 1691-1702, 2020.

26. **Kostidis S, Addie RD, Morreau H, Mayboroda OA and Giera M.** Quantitative NMR analysis of intra-and extracellular metabolism of mammalian cells: A tutorial. *Anal.Chim.Acta* 980: 1-24, 2017.

27. **Lautaoja JH, Lalowski M, Nissinen TA, Hentilä J, Shi Y, Ritvos O, Cheng S and Hulmi JJ.** Muscle and serum metabolomes are dysregulated in colon-26 tumor-bearing mice despite amelioration of cachexia with activin receptor type 2B ligand blockade. *American Journal of Physiology-Endocrinology and Metabolism* 316.5: E852-E865, 2019.

28. **Choudhury R, Beezley J, Davis B, Tomeck J, Gratzl S, Golzarri-Arroyo L, Wan J, Raftery D, Baumes J and O'Connell TM.** Viime: Visualization and Integration of Metabolomics Experiments. *Journal of open source software* 5: 54, 2410, 2020.

29. **Hargreaves M and Spriet LL.** Skeletal muscle energy metabolism during exercise. *Nature Metabolism* 2: 9, 817-828, 2020.

30. **Kramer HF and Goodyear LJ.** Exercise, MAPK, and NF-κB signaling in skeletal muscle. *J.Appl.Physiol.* 103: 1, 388-395, 2007.

31. **Whitham M, Chan MS, Pal M, Matthews VB, Prelovsek O, Lunke S, El-Osta A, Broenneke H, Alber J and Brüning JC.** Contraction-induced interleukin-6 gene

transcription in skeletal muscle is regulated by c-Jun terminal kinase/activator protein-1. *J.Biol.Chem.* 287: 14, 10771-10779, 2012.

32. **Hojman P, Brolin C, Nørgaard-Christensen N, Dethlefsen C, Lauenborg B, Olsen CK, Åbom MM, Krag T, Gehl J and Pedersen BK.** IL-6 release from muscles during exercise is stimulated by lactate-dependent protease activity. *American Journal of Physiology-Endocrinology and Metabolism* 316: 5, E940-E947, 2019.

33. **Romijn JA, Coyle EF, Sidossis LS, Gastaldelli A, Horowitz JF, Endert E and Wolfe RR.** Regulation of endogenous fat and carbohydrate metabolism in relation to exercise intensity and duration. *American Journal of Physiology-Endocrinology and Metabolism* 265: 3, E380-E391, 1993.

34. **Morville T, Sahl RE, Moritz T, Helge JW and Clemmensen C.** Plasma Metabolome Profiling of Resistance Exercise and Endurance Exercise in Humans. *Cell reports* 33: 13, 108554, 2020.

35. **Richter EA and Hargreaves M.** Exercise, GLUT4, and skeletal muscle glucose uptake. *Physiol.Rev.* 93: 3, 993-1017, 2013.

36. **Hirvonen J, Nummela A, Rusko H, Rehunen S and Härkönen M.** Fatigue and changes of ATP, creatine phosphate, and lactate during the 400-m sprint. *Can.J.Sport Sci.* 17: 2, 141-144, 1992.

37. **Burch N, Arnold A, Summermatter S, Santos GBS, Christe M, Boutellier U, Toigo M and Handschin C.** Electric pulse stimulation of cultured murine muscle cells reproduces gene expression changes of trained mouse muscle. *PloS one* 5: 6, e10970, 2010.

38. **Abdelmoez AM, Sardón Puig L, Smith JA, Gabriel BM, Savikj M, Dollet L, Chibalin AV, Krook A, Zierath JR and Pillon NJ.** Comparative profiling of skeletal muscle models reveals heterogeneity of transcriptome and metabolism. *American Journal of Physiology-Cell Physiology 318: 3, C615-C626,* 2019.

39. **Brooks GA.** Lactate as a fulcrum of metabolism. *Redox biology* 101454, 2020.

40. **Tan J, McKenzie C, Potamitis M, Thorburn AN, Mackay CR and Macia L.** The role of short-chain fatty acids in health and disease. *Advances in immunology* 121: 91-119, 2014.

41. **Van Hall G, Sacchetti M and Rådegran G.** Whole body and leg acetate kinetics at rest, during exercise and recovery in humans. *The Journal of Physiology* 542: 1, 263-272, 2002.

42. **Kistner S, Rist MJ, Döring M, Dörr C, Neumann R, Härtel S and Bub A.** An NMR-Based Approach to Identify Urinary Metabolites Associated with Acute Physical Exercise and Cardiorespiratory Fitness in Healthy Humans—Results of the KarMeN Study. *Metabolites* 10: 5, 212, 2020.

43. **Knowles SE, Jarrett IG, Filsell OH and Ballard FJ.** Production and utilization of acetate in mammals. *Biochem.J.* 142: 2, 401-411, 1974.

44. **Liu X, Cooper DE, Cluntun AA, Warmoes MO, Zhao S, Reid MA, Liu J, Lund PJ, Lopes M and Garcia BA.** Acetate production from glucose and coupling to mitochondrial metabolism in mammals. *Cell* 175: 2, 502-513. e13, 2018.

45. **Spriet LL and Heigenhauser GJ**. Regulation of pyruvate dehydrogenase (PDH) activity in human skeletal muscle during exercise. *Exerc.Sport Sci.Rev* 30: 2, 91-95, 2002.

46. **Liu L, Fu C and Li F.** Acetate affects the process of lipid metabolism in rabbit liver, skeletal muscle and adipose tissue. *Animals* 9: 10, 799, 2019.

47. **Kamphorst JJ, Chung MK, Fan J and Rabinowitz JD.** Quantitative analysis of acetyl-CoA production in hypoxic cancer cells reveals substantial contribution from acetate. *Cancer & Metabolism* 2: 1, 1-8, 2014.

48. **Frampton J, Murphy KG, Frost G and Chambers ES.** Short-chain fatty acids as potential regulators of skeletal muscle metabolism and function. *Nature metabolism* 1-9, 2020.

49. **Pillon NJ, Gabriel BM, Dollet L, Smith JA, Puig LS, Botella J, Bishop DJ, Krook A and Zierath JR.** Transcriptomic profiling of skeletal muscle adaptations to exercise and inactivity. *Nature communications* 11: 1, 1-15, 2020.

50. **Klein DJ, McKeever KH, Mirek ET and Anthony TG.** Metabolomic response of equine skeletal muscle to acute fatiguing exercise and training. *Frontiers in physiology* 11: 110, 2020.

51. **Contrepois K, Wu S, Moneghetti KJ, Hornburg D, Ahadi S, Tsai M, Metwally AA, Wei E, Lee-McMullen B and Quijada JV.** Molecular Choreography of Acute Exercise. *Cell* 181: 5, 1112-1130, e16, 2020.

52. **Blomstrand E and Essén-Gustavsson B.** Changes in amino acid concentration in plasma and type I and type II fibres during resistance exercise and recovery in human subjects. *Amino Acids* 37: 4, 629, 2009.

53. **Kainulainen H, Hulmi JJ and Kujala UM.** Potential role of branched-chain amino acid catabolism in regulating fat oxidation. *Exerc.Sport Sci.Rev.* 41: 4, 194-200, 2013.

54. **Tipton KD, Hamilton DL and Gallagher IJ.** Assessing the role of muscle protein breakdown in response to nutrition and exercise in humans. *Sports Medicine* 48: 1, 53-64, 2018.

55. **Dhanani ZN, Mann G and Adegoke OA.** Depletion of branched-chain aminotransferase 2 (BCAT2) enzyme impairs myoblast survival and myotube formation. *Physiological reports* 7: 23, e14299, 2019.

56. **Bekeova C, Anderson-Pullinger L, Boye K, Boos F, Sharpadskaya Y, Herrmann JM and Seifert EL.** Multiple mitochondrial thioesterases have distinct tissue and substrate specificity and CoA regulation, suggesting unique functional roles. *J.Biol.Chem* 294: 50, 19034-19047, 2019.

57. **Zhou L, Wang L, Lu L, Jiang P, Sun H and Wang H.** Inhibition of miR-29 by TGF-beta-Smad3 signaling through dual mechanisms promotes transdifferentiation of mouse myoblasts into myofibroblasts. *PLoS One* 7: 3, e33766, 2012.

58. **Tillander V, Nordström EA, Reilly J, Strozyk M, Van Veldhoven PP, Hunt MC and Alexson SE.** Acyl-CoA thioesterase 9 (ACOT9) in mouse may provide a novel link between fatty acid and amino acid metabolism in mitochondria. *Cellular and molecular life sciences* 71: 5, 933-948, 2014.

59. **Peake JM, Tan SJ, Markworth JF, Broadbent JA, Skinner TL and Cameron-Smith D.** Metabolic and hormonal responses to isoenergetic high-intensity interval exercise and continuous moderate-intensity exercise. *American Journal of Physiology-Endocrinology and Metabolism* 307: 7, E539-E552, 2014.

60. **Hoshino D, Kawata K, Kunida K, Hatano A, Yugi K, Wada T, Fujii M, Sano T, Ito Y and Furuichi Y.** Trans-omic analysis reveals ROS-dependent pentose phosphate pathway activation after high-frequency electrical stimulation in C2C12 myotubes. *Iscience* 23: 10, 101558, 2020.

61. **Saddik M, Gamble J, Witters LA and Lopaschuk GD.** Acetyl-CoA carboxylase regulation of fatty acid oxidation in the heart. *J.Biol.Chem* 268: 34, 25836-25845, 1993.

62. **Laurens C, Bourlier V, Mairal A, Louche K, Badin P, Mouisel E, Montagner A, Marette A, Tremblay A and Weisnagel JS.** Perilipin 5 fine-tunes lipid oxidation to metabolic demand and protects against lipotoxicity in skeletal muscle. *Scientific reports* 6: 38310, 2016.

63. **Li L, Ma J, Li S, Chen X and Zhang J.** Electric pulse stimulation inhibited lipid accumulation on C2C12 myotubes incubated with oleic acid and palmitic acid. *Arch.Physiol.Biochem.* 1-7, 2019.

64. **Nikolić N, Bakke SS, Kase ET, Rudberg I, Halle IF, Rustan AC, Thoresen GH and Aas V.** Electrical pulse stimulation of cultured human skeletal muscle cells as an in vitro model of exercise. *PLoS One* 7: 3. e33203, 2012.

65. **Lambernd S, Taube A, Schober A, Platzbecker B, Görgens SW, Schlich R, Jeruschke K, Weiss J, Eckardt K and Eckel J.** Contractile activity of human skeletal muscle cells prevents insulin resistance by inhibiting pro-inflammatory signalling pathways. *Diabetologia* 55: 4, 1128-1139, 2012.

66. **Marš T, Miš K, Meznarič M, Prpar Mihevc S, Vid J, Haugen F, Rogelj B, Raustan AC, Thoresen GH, Pirkmajer S and Nikolić N.** Innervation and electrical pulse

stimulation–in vitro effects on human skeletal muscle cells. *Applied Physiology, Nutrition, and Metabolism* 99: 999, 1-10, 2020.

67. **Lessard SJ, MacDonald TL, Pathak P, Han MS, Coffey VG, Edge J, Rivas DA, Hirshman MF, Davis RJ and Goodyear LJ.** JNK regulates muscle remodeling via myostatin/SMAD inhibition. *Nature communications* 9: 1, 3030, 2018.

68. **Hentilä J, Ahtiainen JP, Paulsen G, Raastad T, Häkkinen K, Mero AA and Hulmi JJ.** Autophagy is induced by resistance exercise in young men, but unfolded protein response is induced regardless of age. *Acta physiologica* 224: 1, e13069, 2018.

69. **MacDonald TL, Pattamaprapanont P, Pathak P, Fernandez N, Freitas EC, Hafida S, Mitri J, Britton SL, Koch LG and Lessard SJ.** Hyperglycaemia is associated with impaired muscle signalling and aerobic adaptation to exercise. *Nature Metabolism* 2: 9, 902-917, 2020.

70. **Théry C, Witwer KW, Aikawa E, Alcaraz MJ, Anderson JD, Andriantsitohaina R, Antoniou A, Arab T, Archer F and Atkin-Smith GK.** Minimal information for studies of extracellular vesicles 2018 (MISEV2018): a position statement of the International Society for Extracellular Vesicles and update of the MISEV2014 guidelines. *Journal of extracellular vesicles* 7: 1, 1535750, 2018.

71. **Marshall DD and Powers R.** Beyond the paradigm: Combining mass spectrometry and nuclear magnetic resonance for metabolomics. *Prog Nucl Magn Reson Spectrosc* 100: 1-16, 2017.

72. **Hui S, Cowan AJ, Zeng X, Yang L, TeSlaa T, Li X, Bartman C, Zhang Z, Jang C and Wang L.** Quantitative fluxomics of circulating metabolites. *Cell metabolism* 32: 4, 676-688. e4, 2020.

Higher glucose availability augments the metabolic responses of the C2C12 myotubes to exercise-like electrical pulse stimulation

METHODS

C2C12 myotubes

± 24h EL-EPS (1 Hz, 2 ms, 12V)

Low glucose (1.0 g/l)

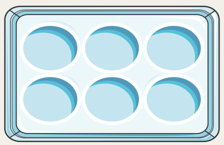

High glucose (4.5 g/l)

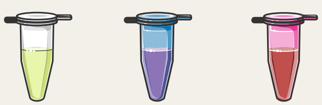

Cells **Media** **Cell-free media**

- NMR metabolome
- Signaling pathways
- Cytokine secretion
- Oleate oxidation
- Exerkine effects

OUTCOME

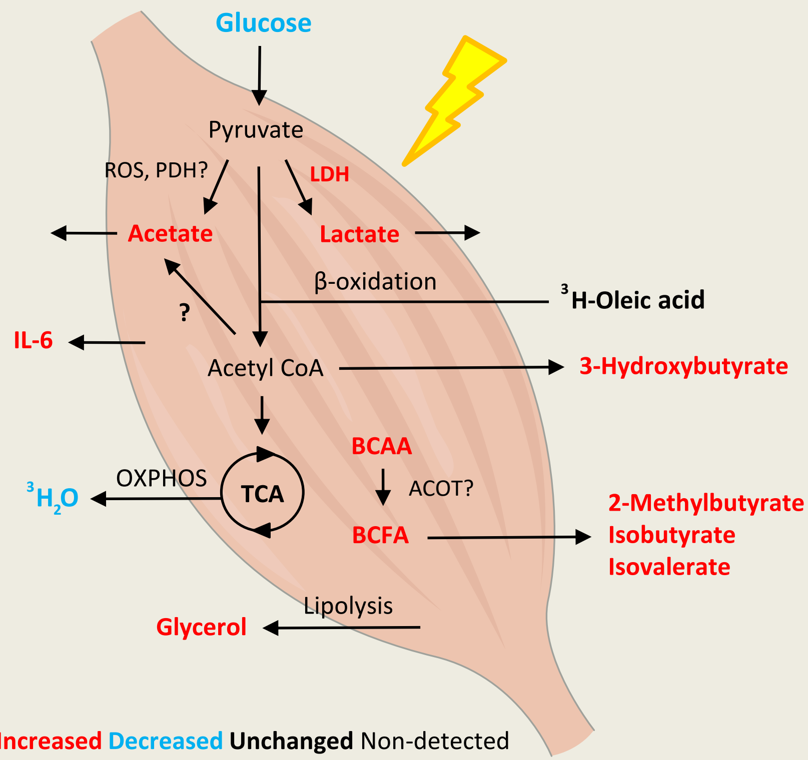

Increased Decreased **Unchanged** Non-detected

CONCLUSION

EL-EPS induced:

- ATP production via glucose, phosphocreatine and lactate metabolism
- Greater responses on metabolites under high glucose condition
- BCAA catabolism and BCFA secretion
- Release of acetate and 3-hydroxybutyrate
- No effects on the cell-free media

Figure 1


A
Cells
Medium
PC1 (25 %)
PC2 (15 %)
PC1 (27 %)
PC2 (16 %)
LG
LG + EPS
HG
HG + EPS
B
Cells
Medium
13
24
10
24 common metabolites
2-Methylbutyrate
Acetate
Alanine
Arginine
Citrate
Creatine
Formate
Fumarate
Glucose
Glutamate
Glutamine
Glycine
Isobutyrate
Isoleucine
Isovalerate
Lactate
Leucine
Lycine
myo-Inositol
Phenylalanine
Succinate
Thre onine
Tyrosine
Valine
C
3
14
24
6
Energy related metabolites
SCFAs, BCFAs and ketone bodies
AAs and related metabolites
Vitamins and others
D
Cells
-3.3
0
3.3
EPS
HG
LG
Isoleucine
Valine
Phenylalanine
Tyrosine
Leucine
Threonine
Glutamine
Lysine
Arginine
myo-Inositol
Guanidoacetate
Alanine
Glycine
β-Alanine
Creatine
Isovalerate
2-Methylbutyrate
Isobutyrate
Succinate
Citrate
Adenosine diphosphate
Acetate
Propionate
Malate
Fumarate
Lactate
Glucose
Pantothenate
Phosphocreatine
Formate
O-Phosphocholine
Glutamate
Aspartate
Taurine
sn-Glycero-3-phosphocholine
NAD+
UDP-glucose
LG
LG+EPS
HG
HG+EPS
E
Medium
-3.2
0
3.2
Inconsistent EPS
HG + EPS
LG
EPS
HG
Isoleucine
Valine
Leucine
Phenylalanine
Tryptophan
Citrate
Formate
Pyroglutamate
Glycine
Lysine
Asparagine
Cystine
Pyridoxine
Lactate
Alanine
Threonine
Isobutyrate
Isovalerate
2-Methylbutyrate
Creatine
Histidine
Glutamate
Choline
Ethanol
Arginine
Tyrosine
Acetate
3-Hydroxybutyrate
Succinate
Glucose
Fumarate
myo-Inositol
Serine
Glutamine
LG
LG+EPS
HG
HG+EPS

Figure 2

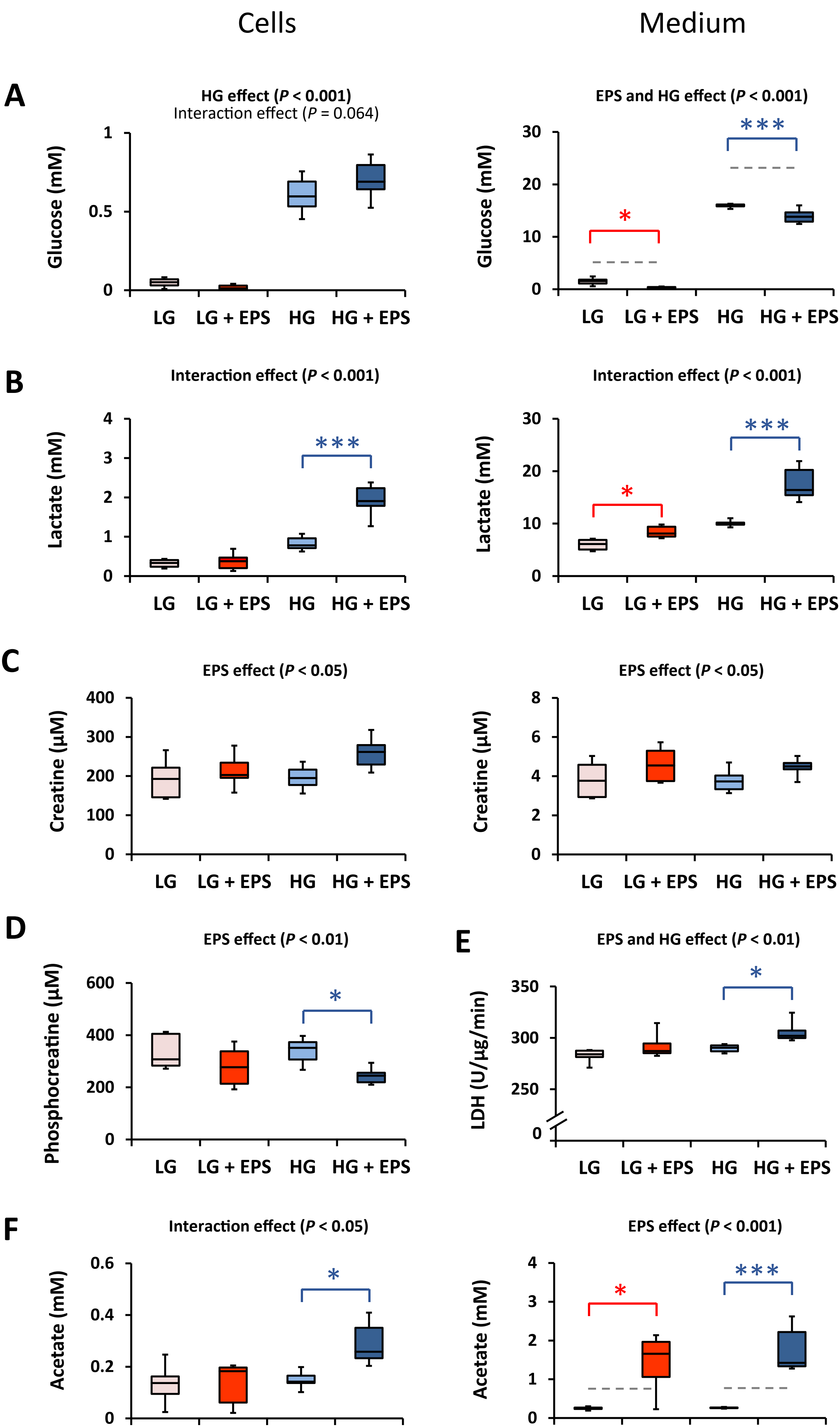
Cells
Medium
A
HG effect (P < 0.001)
Interaction effect (P = 0.064)
Glucose (mM)
EPS and HG effect (P < 0.001)
Glucose (mM)
B
Interaction effect (P < 0.001)
Lactate (mM)
Interaction effect (P < 0.001)
Lactate (mM)
C
EPS effect (P < 0.05)
Creatine (µM)
EPS effect (P < 0.05)
Creatine (µM)
D
EPS effect (P < 0.01)
Phosphocreatine (µM)
E
EPS and HG effect (P < 0.01)
LDH (U/µg/min)
F
Interaction effect (P < 0.05)
Acetate (mM)
EPS effect (P < 0.001)
Acetate (mM)
LG
LG + EPS
HG
HG + EPS
*
***

Figure 3

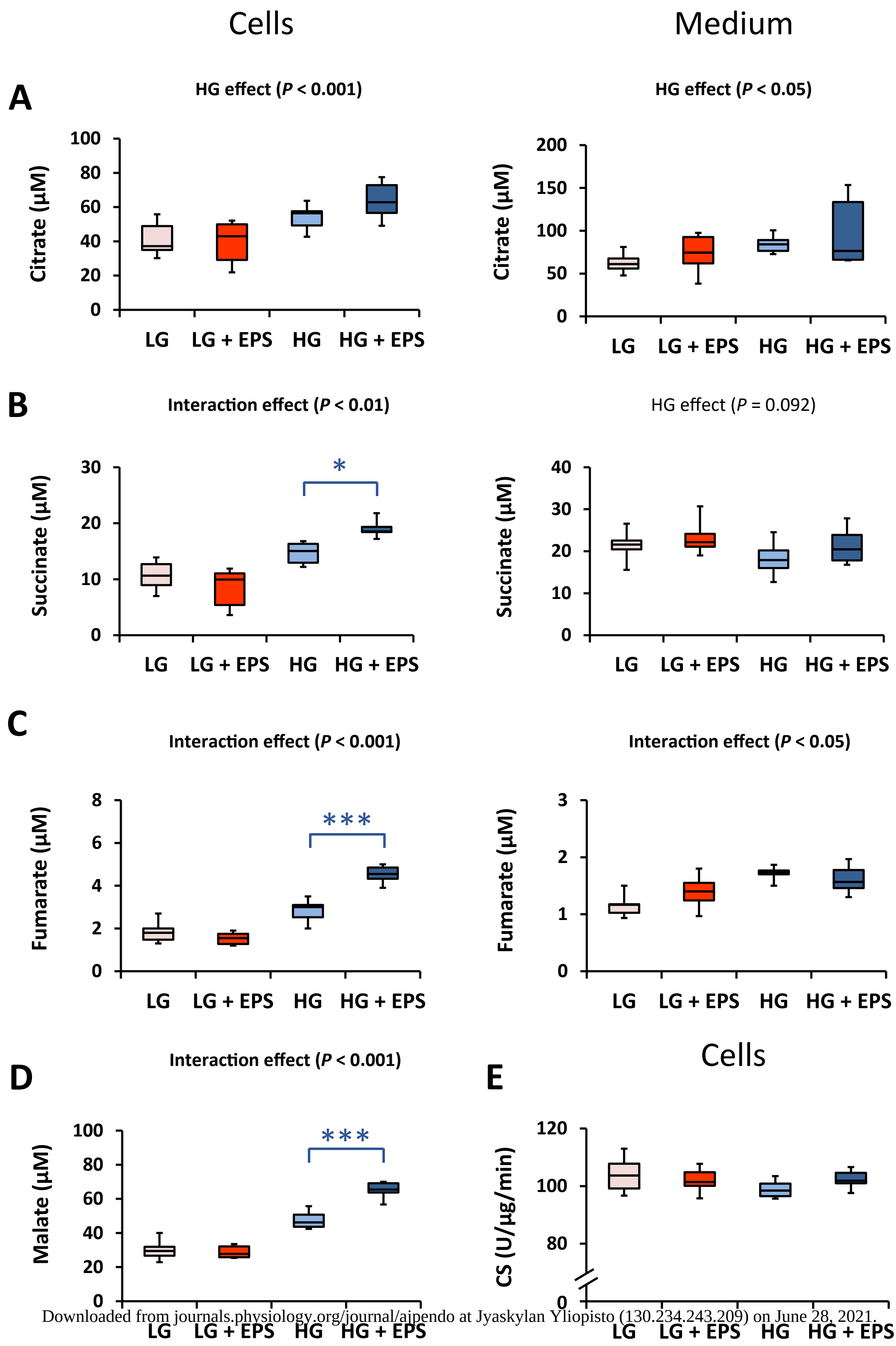

Cells
Medium
A
HG effect (P < 0.001)
Citrate (µM)
100
80
60
40
20
0
LG
LG + EPS
HG
HG + EPS
HG effect (P < 0.05)
Citrate (µM)
200
150
100
50
0
LG
LG + EPS
HG
HG + EPS
B
Interaction effect (P < 0.01)
Succinate (µM)
30
20
10
0
*
LG
LG + EPS
HG
HG + EPS
HG effect (P = 0.092)
Succinate (µM)
40
30
20
10
0
LG
LG + EPS
HG
HG + EPS
C
Interaction effect (P < 0.001)
Fumarate (µM)
8
6
4
2
0
***
LG
LG + EPS
HG
HG + EPS
Interaction effect (P < 0.05)
Fumarate (µM)
3
2
1
0
LG
LG + EPS
HG
HG + EPS
D
Interaction effect (P < 0.001)
Malate (µM)
100
80
60
40
20
0
***
LG
LG + EPS
HG
HG + EPS
E
Cells
CS (U/µg/min)
120
100
80
0
LG
LG + EPS
HG
HG + EPS

Figure 4

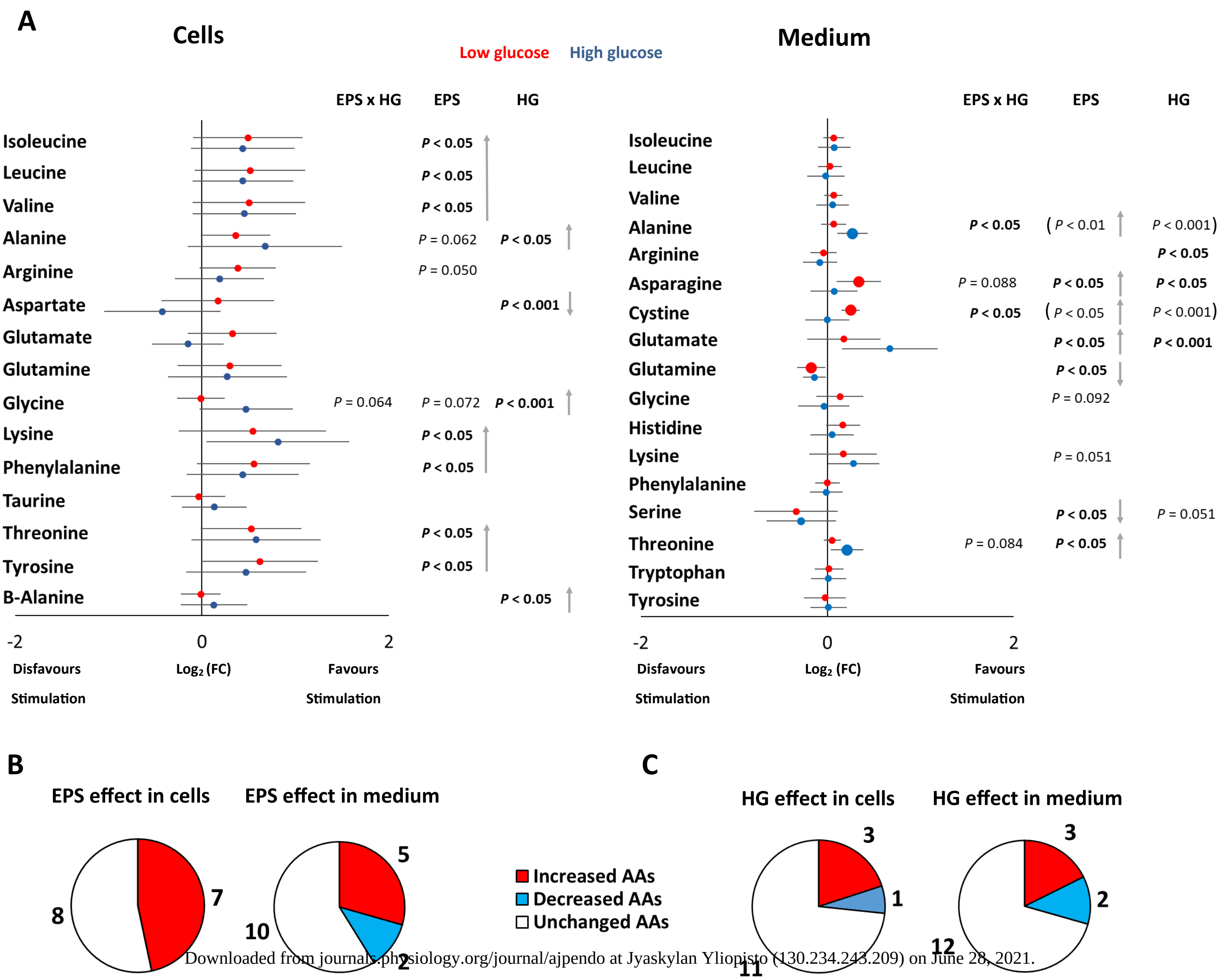

A
Cells
Low glucose
High glucose
Medium
EPS x HG
EPS
HG
Isoleucine
Leucine
Valine
Alanine
Arginine
Aspartate
Glutamate
Glutamine
Glycine
Lysine
Phenylalanine
Taurine
Threonine
Tyrosine
B-Alanine
P < 0.05
P = 0.062
P = 0.050
P < 0.001
P = 0.064
P = 0.072
Cystine
Histidine
Serine
Tryptophan
Asparagine
P < 0.01
P < 0.001
P = 0.088
P = 0.092
P = 0.051
P = 0.084
-2
0
2
Disfavours
Stimulation
Log2 (FC)
Favours
Stimulation
B
EPS effect in cells
EPS effect in medium
8
7
10
5
2
Increased AAs
Decreased AAs
Unchanged AAs
C
HG effect in cells
HG effect in medium
3
1
11
3
2
12

Figure 5

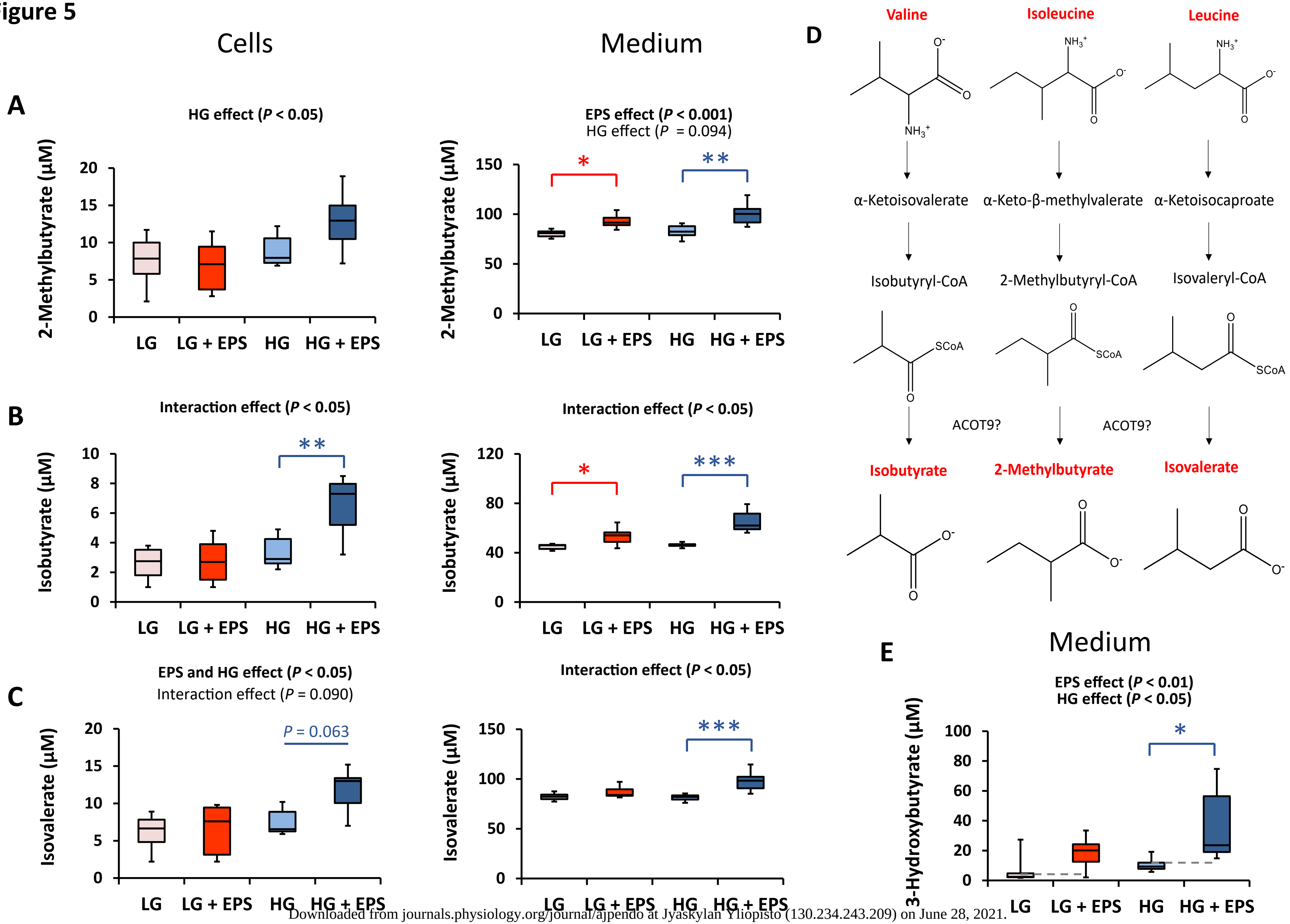

Cells
Medium
A
HG effect (P < 0.05)
2-Methylbutyrate (µM)
EPS effect (P < 0.001)
HG effect (P = 0.094)
*
**
LG
LG + EPS
HG
HG + EPS
B
Interaction effect (P < 0.05)
Isobutyrate (µM)
**
Interaction effect (P < 0.05)
*
***
C
EPS and HG effect (P < 0.05)
Interaction effect (P = 0.090)
Isovalerate (µM)
P = 0.063
Interaction effect (P < 0.05)
***
D
Valine
Isoleucine
Leucine
α-Ketoisovalerate
α-Keto-β-methylvalerate
α-Ketoisocaproate
Isobutyryl-CoA
2-Methylbutyryl-CoA
Isovaleryl-CoA
SCoA
ACOT9?
ACOT9?
Isobutyrate
2-Methylbutyrate
Isovalerate
E
Medium
EPS effect (P < 0.01)
HG effect (P < 0.05)
3-Hydroxybutyrate (µM)
*

Figure 6

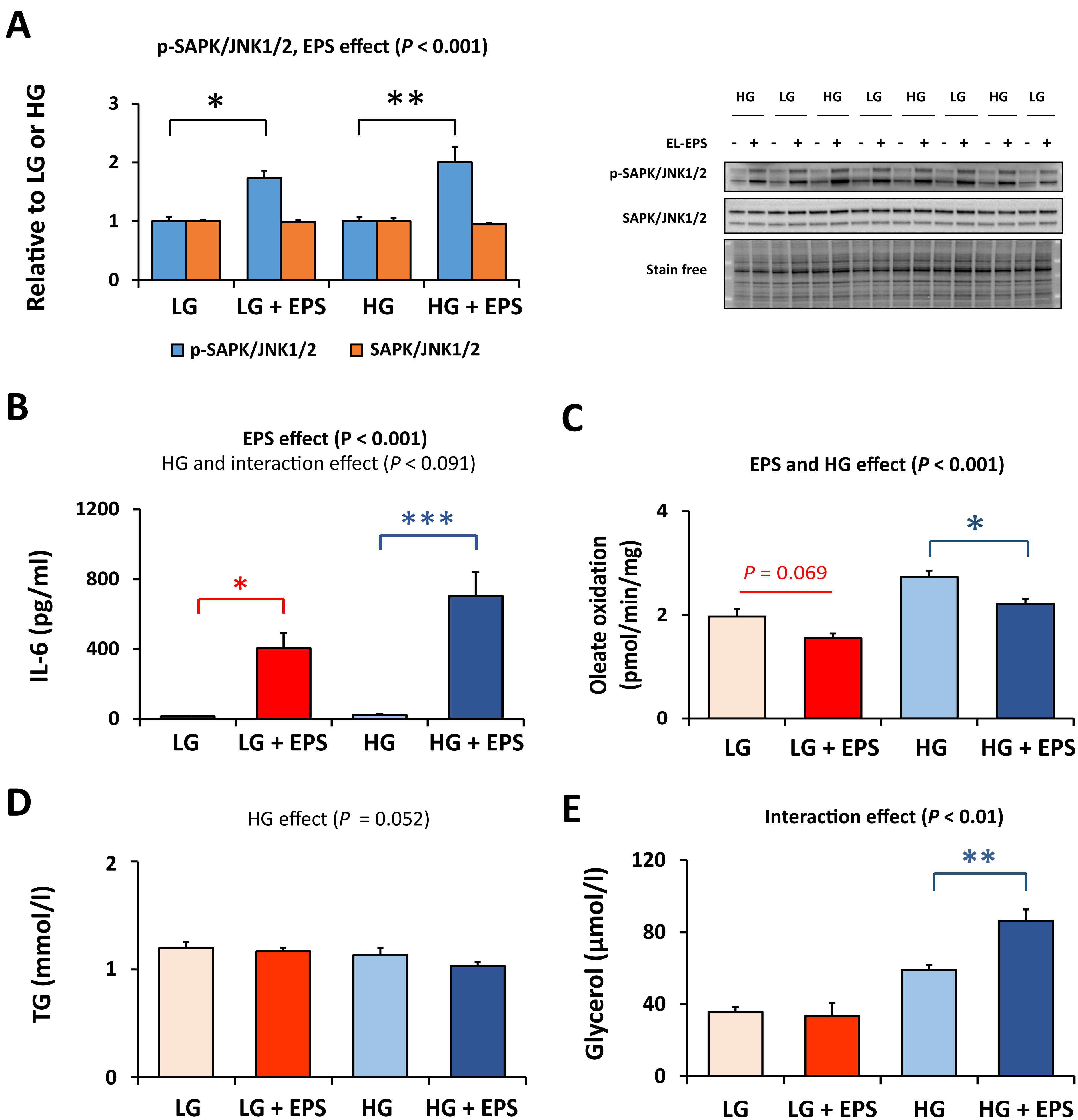
A
p-SAPK/JNK1/2, EPS effect (P < 0.001)
Relative to LG or HG
3
2
1
0
*
**
LG
LG + EPS
HG
HG + EPS
p-SAPK/JNK1/2
SAPK/JNK1/2
HG LG HG LG HG LG HG LG
EL-EPS
- + - + - + - + - + - + - + - +
p-SAPK/JNK1/2
SAPK/JNK1/2
Stain free
B
EPS effect (P < 0.001)
HG and interaction effect (P < 0.091)
IL-6 (pg/ml)
1200
800
400
0
*
***
LG
LG + EPS
HG
HG + EPS
C
EPS and HG effect (P < 0.001)
Oleate oxidation (pmol/min/mg)
4
2
0
P = 0.069
*
LG
LG + EPS
HG
HG + EPS
D
HG effect (P = 0.052)
TG (mmol/l)
2
1
0
LG
LG + EPS
HG
HG + EPS
E
Interaction effect (P < 0.01)
Glycerol (µmol/l)
120
80
40
0
**
LG
LG + EPS
HG
HG + EPS

Figure 7

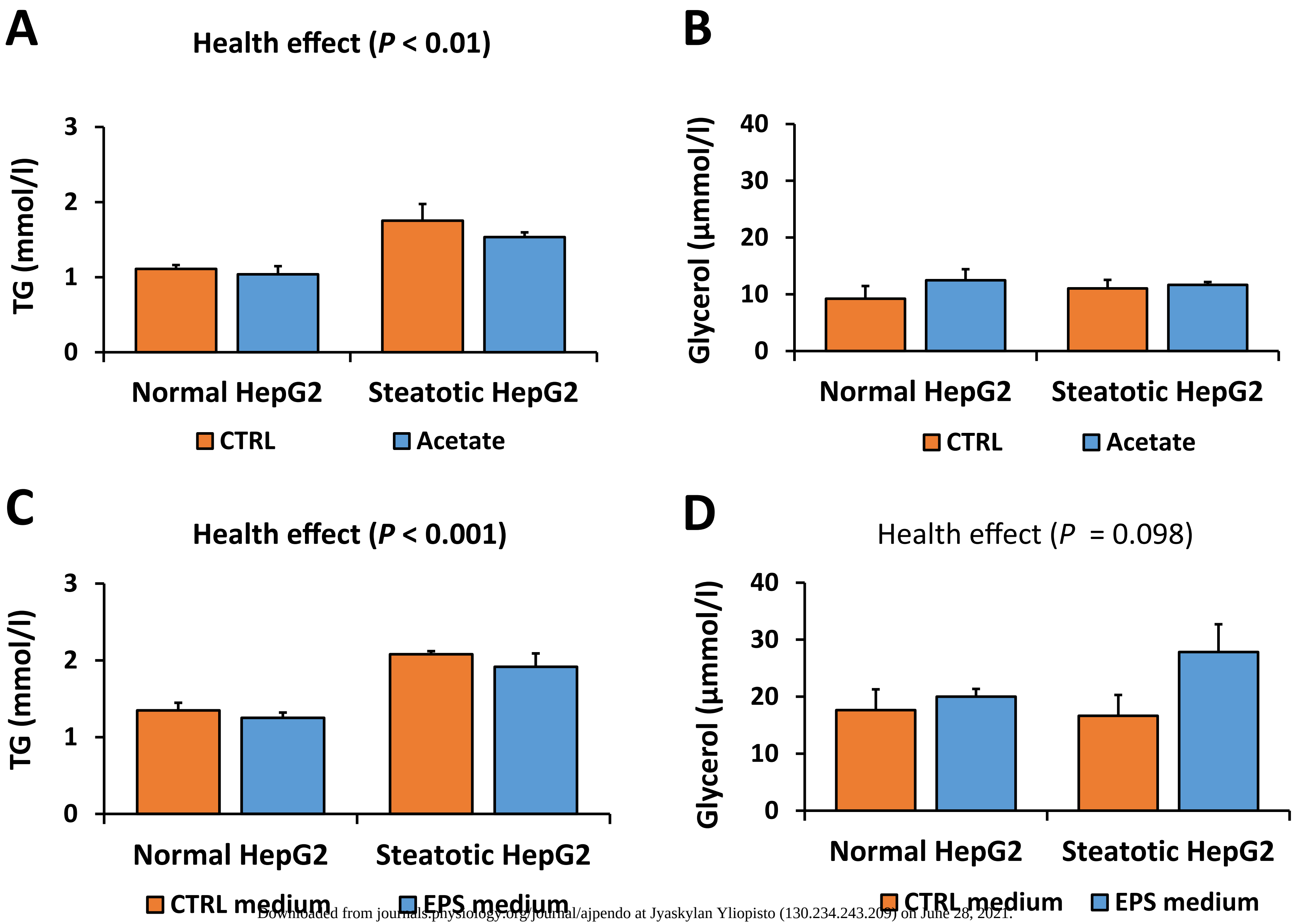
A
Health effect (P < 0.01)
TG (mmol/l)
3
2
1
0
Normal HepG2
Steatotic HepG2
CTRL
Acetate
B
Glycerol (µmmol/l)
40
30
20
10
0
Normal HepG2
Steatotic HepG2
CTRL
Acetate
C
Health effect (P < 0.001)
TG (mmol/l)
3
2
1
0
Normal HepG2
Steatotic HepG2
CTRL medium
EPS medium
D
Health effect (P = 0.098)
Glycerol (µmmol/l)
40
30
20
10
0
Normal HepG2
Steatotic HepG2
CTRL medium
EPS medium

Figure 8

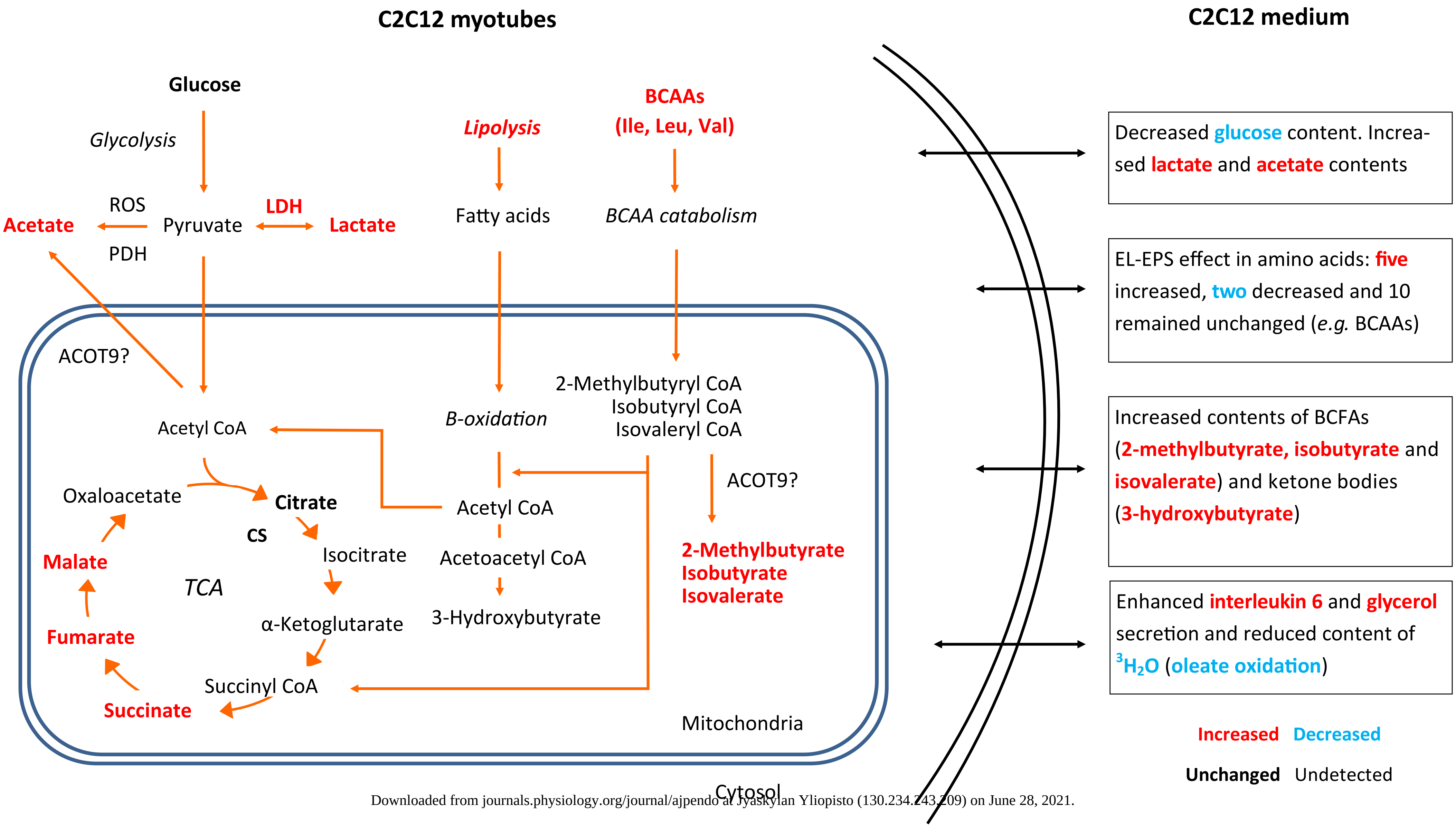
C2C12 myotubes
C2C12 medium
Glucose
Glycolysis
Lipolysis
BCAAs
(Ile, Leu, Val)
ROS
PDH
LDH
Acetate
Pyruvate
Lactate
Fatty acids
BCAA catabolism
ACOT9?
Acetyl CoA
B-oxidation
2-Methylbutyryl CoA
Isobutyryl CoA
Isovaleryl CoA
Oxaloacetate
Citrate
CS
Acetyl CoA
ACOT9?
Isocitrate
Acetoacetyl CoA
Malate
TCA
2-Methylbutyrate
Isobutyrate
Isovalerate
α-Ketoglutarate
3-Hydroxybutyrate
Fumarate
Succinyl CoA
Succinate
Mitochondria
Cytosol
Decreased glucose content. Increased lactate and acetate contents
EL-EPS effect in amino acids: five increased, two decreased and 10 remained unchanged (e.g. BCAAs)
Increased contents of BCFAs (2-methylbutyrate, isobutyrate and isovalerate) and ketone bodies (3-hydroxybutyrate)
Enhanced interleukin 6 and glycerol secretion and reduced content of ³H₂O (oleate oxidation)
Increased
Decreased
Unchanged
Undetected